THE FUNCTIONS OF FE65 PROTEINS AND THEIR ROLES IN DEMENTIAS OF THE ALZHEIMER TYPE

by

Baiping Wang

A dissertation submitted in partial fulfillment

of the requirements of the degree of

Doctor of Philosophy

University of Washington

2003

Program Authorized to Offer Degree: Pathology

UMI Number: 3102731

UMI Microform 3102731

ProQuest Information and Learning Company
300 North Zeeb Road
P.O. Box 1346
Ann Arbor, MI 48106-1346

In presenting this dissertation in partial fulfillment of the requirements for the Doctoral degree at the University of Washington, I agree that the Library shall make its copies freely available for inspection. I further agree that extensive copying of the dissertation is allowable only for scholarly purposes, consistent with "fair use" as prescribed in the U.S. Copyright Law. Requests for copying or reproduction of this dissertation may be referred to Bell and Howell Information and Learning, 300 North Zeeb Road, P.O. Box 1346, Ann Arbor, MI 48106-1346, to whom the author has granted "the right to reproduce and sell (a) copies of the manuscript in microform and/or (b) printed copies of the manuscript made from microform."

Signature 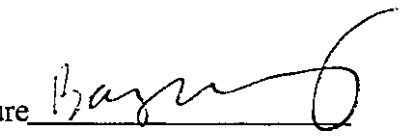

Date Aug 19 2003

University of Washington

Graduate School

This is to certify that I have examined this copy of doctoral dissertation by

Baiping Wang

and have found that it is complete and satisfactory in all respects,

and that any and all revisions required by the final

examining committee have been made.

Chair of Supervisory Committee:

George M. Martin

Reading Committee:

George M. Martin

Quibai Hu

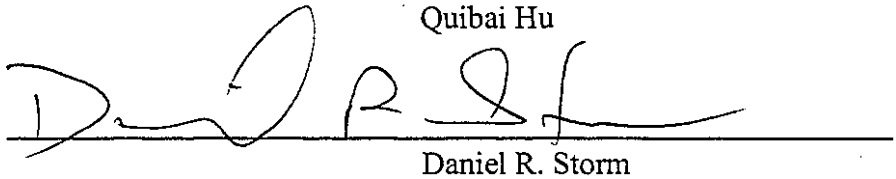

Daniel R. Storm

Date:

8/19/2003

University of Washington

Abstract

The functions of FE65 proteins and their roles in the Dementia of Alzheimer type

Baiping Wang

Chairperson of the Supervisory Committee

Professor George M. Martin

Department of Pathology

Dementias of the Alzheimer type (DAT) are human neurodegenerative diseases that debilitate millions of elderly people, presenting enormous financial and emotional burdens worldwide. Its pathogenesis involves the beta-amyloid precursor protein (βPP), the aberrant processing or functioning of which results in amyloid plaques, the hallmark of DAT pathology. Attempts to decipher their normal function and metabolism of βPP have focused on the interacting proteins. A particularly strong interactor, the FE65 protein, has properties of an adaptor protein. An understanding of its functions may elucidate the molecular mechanisms underlying the pathogenesis of DAT.

This thesis focuses on the functions of FE65 and its role in DAT. Using a gene-targeting approach, FE65 was disrupted in transgenic mice. These mice were bred with a line of transgenic mice (Tg2576) that overexpress a mutant form of βPP, resulting in extensive deficits of beta amyloid.

After documenting the successful targeting of *FE65*, a Western analysis of FE65 protein expression was carried out with a panel of FE65-specific antibodies. These demonstrated that the 97 kDa full-length FE65 (p97) was ablated in the mutant mice while a previously undescribed FE65 isoform with apparent molecular mass of 60 kDa (p60) was expressed in both wild type and mutant mice. p60 has a truncated N-terminus, and is likely to be generated through alternative translation. Expressions of the two isoforms appeared to be brain-region distinct, and age-dependent. The mutant mice were viable, and showed no obvious physical impairments or histopathological abnormalities. However, homozygous ($p97FE65^{-/-}$) and heterozygous ($p97FE65^{+/-}$) mutant mice exhibited poorer performances than wild type mice on a passive avoidance task when tested at 14 months. $p97FE65^{-/-}$ mice at 14 months also exhibit impaired hidden-platform acquisition and a severe reversal-learning deficit, but normal visual-platform acquisition in the Morris water maze tests. Probe trials confirmed impairments in $p97FE65^{-/-}$ mice in re-learning of new spatial information, suggesting a hippocampal-dependent memory extinction deficit. Reduced secretion

of Aβ peptides was observed in primary neuronal cultures of hybrid mice (p97FE65$^{-/-}$ /Tg2576).

These studies suggest an important and novel function of FE65 in learning and memory.

TABLE OF CONTENTS

List of Figures iv

List of Tables v

List of Abbreviations vi

Chapter 1: Introduction 1

1.1. Overview 1

1.2. Dementias of the Alzheimer type (DAT) 2

1.2.1. Genetics of DAT 2

1.2.2. Pathology of DAT 3

1.2.3. DAT pathogenesis: Amyloid hypothesis 3

1.3. The beta-Amyloid Precursor Protein (βPP) 4

1.3.1. βPP metabolism 4

1.3.2. βPP function 6

1.3.3. βPP binding proteins 8

1.4. FE65- An Adaptor Protein 9

1.4.1. FE65 Domain Structures and Binding Proteins 9

1.4.2. FE65 Family 12

1.4.3. FE65 Functions 13

1.4.4. The Role of FE65 in DAT 14

Chapter 2: Generation and phenotypic characterization of of Isoform- Specific FE65 knockout mice 18

2.1. Introduction 18

2.2. Materials and Methods 19

2.2.1. Determination of the Mouse FE65 cDNA Sequence 20

2.2.2. Construction of a FE65 Gene Targeting Vector 20

2.2.3. Selection of Homologous Recombinant ES Cell Clones and Production of Mutant Mice 21

2.2.4. Northern Analysis and RT-PCR 22

2.2.5. Western Analysis 23

2.2.6. Histopathological Studies 24

2.2.7. Neuronal Cultures 24

2.2.8. Aβ Quantitation 25

2.3. Results 25

2.3.1. Molecular Characterization of FE65 Mutant Mice 26

2.3.1.1. Northern analysis and RT-PCR 26

2.3.1.2. Western Analysis and GST-βPP-C48 Pull Down Assays 27

2.3.1.3. Evidence for Normal Expression of FE65 L1/L2 28

2.3.1.4. Evidence for Normal Expression of FE65-Binding Proteins 29

2.3.2. Physical Characterization of FE65 Mutant Mice 29

2.3.2.1. General Characterization 29

2.3.2.2. Normal anatomy 29

2.3.2.3. Normal lifespan 30

2.3.2.4. Decreased fertilities 30

2.3.3. Crosses of FE65 mutant mice with Tg2576 mice 30

2.3.3.1. Decreased survival rates for Tg2576 X FE65 F1 hybrid mice 31

2.3.2.2. Reduced generation of Aβ peptides in Primary Neuronal Cultures of Tg2576 X FE65 F1 hybrid mice..... 32

2.4. Discussion 32

Chapter 3: Identification and Characterization of a Novel Isoform of FE65 Protein 45

3.1. Introduction 45

3.2. Materials and Methods 46

3.3.1. Western Analysis and GST Pull Down Assays..... 46

3.3.2. Cytoplasmic and Nuclear Fractionation 46

3.3. Results 47

3.3.1. Identification of a Novel Isoform of FE65 Proteins (p60) 47

3.3.2. Increased Binding Affinity of p60 for the beta amyloid precursor protein intracellulor domain (AICD) 49

3.3.3. Differential Expression of FE65 Isoforms In Vitro 49

3.3.4. Cytoplasmic Localization of p60 49

3.3.5. Brain-Region Specific Expression of p60 50

3.3.6. Age-Related Expression of FE65 Isoforms 51

3.3.7. Tissue Distributions of FE65 Isoforms 51

3.4. Discussion 51

Chapter 4: Behavioral Analysis of FE65 Mutant Mice 62

4.1. Introduction 62

4.2. Materials and Methods 62

4.3.1. Animals 62

4.3.2. Open Field Test 63

4.3.3. Passive Avoidance Learning 63

4.3.4. Morris Water Maze (MWM) 64

4.3.5. Statistics 66

4.3. Results 67

4.3.1. Normal Performance in the Open Field Test 67

4.3.2. Impaired Passive Avoidance Learning 68

4.3.3. Impaired Performance in the Morris Water Maze 69

4.4. Discussion 74

Chapter 5 Conclusions and Future Directions. 83

5.1 Conclusions and Implications 83

5.2 Future Directions 86

5.2.1. Gene Expression Profiling by Microarray and Quantitive RT-PCR 86

5.2.2. Role of FE65 in Synaptic Plasticity 86

Bibiography 88

LIST OF FIGURES

Figure Number Page

1.1 Proteolysis of βPP 16

1.2 The FE65 interacting protein network..... 17

2.1 Amino-acid sequence comparison of human, rat and mouse FE65 proteins. 35

2.2 Procedure for generating transgenic mice via gene targeting..... 36

2.3 Schematic diagram of the pNTK2 targeting vector and the FE65 genomic clone 37

2.4. *FE65* gene structure and gene targeting strategy 38

2.5 Southern and PCR analysis of the targeted gene..... 39

2.6 Northern and RT-PCR analysis of *FE65* transcripts 40

2.7 Western Analysis of FE65 proteins from crude lysates of mouse brain 41

2.8 Expressions of FE65 binding proteins and X11α in FE65 mutant mice..... 42

2.9 Survival analysis of Tg2576 X*FE65* F1 hybrid mice. 43

2.10 Quantitation of Aβ peptides in media from primary neuronal cultures of Tg2576X FE65 F1 hybrid mice..... 44

3.1 Western and GST-pulldown analyses of expressions of FE65 isoforms 56

3.2 Brain region-specific expressions of p60 57

3.3 Expression of FE65 isoforms during development and aging..... 58

3.4 Subcellular localizations of endogenous FE65 proteins in mouse brains 69

3.5 Tissue Distributions of FE65 isoforms..... 60

4.1 Common learning tests 78

4.2 Measures of locomotor activity and open field behavior 79

4.3 Performance of FE65 mutant mice in a passive avoidance test 80

4.4 Performance of FE65 mutant mice in the Morris water maze..... 81

4.5 Performance of FE65 mutant mice in probe tests 82

5.1 A simplified model of gene actions involving a segment of the FE65 protein networks. 87

LIST OF TABLES

Table Number Page

1. Survey of ATG Codons and Their Flanking Nucleotides Within the First 1200 Nucleotides of the p97FE65 cDNA..... 61

LIST OF ABBREVIATIONS

Aβ	β-amyloid
Abl	Abelson oncogene with tyrosine kinase activity
AICD	[beta]-amyloid precursor protein intracellular domain
APP	the βPP gene
βPP	[beta]-amyloid precursor protein
βPPs	the secreted form of βPP
ECL	enhanced chemiluminescence
ES cell	Embryonic stem cell
DAT	Dementias of the Alzheimer type
mDab	mammalian orthologue of *Drosophila* disabled
FE65	the FE65 gene
FE65	the FE65 protein
FE65L1	FE65-like protein1
FE65L2	FE65-like protein 2
GST	glutathione S-transferase
HRP	Horseradish peroxidase
IRES	Internal ribosomal entry site
LRP	low- density lipoprotein receptor- related protein
LTP	long term potentiation

Mena	mammalian homologue of Drosophila enabled protein
MWM	Morris water maze
NFT	neurofibrillary tangles
PAGE	polyacrylamide gel electrophoresis
PBS	phosphate buffered saline
PCR	polymerase chain reaction
PID	phosphotyrosine interacting domain
PS	Presenilin
RT	reverse transcriptase
Tip60	a histone acetyltransferase
Tg 2576	mutant *APP* transgenic mice Tg(HuAPP695.SWE)2576
WW domain	a protein module with two conserved tryptophans

ACKNOWLEDGMENTS

Many thanks to my advisor Dr. George Martin who provided me this opportunity and encouraged me through these years. Without his support for independent research and his encouragement, this work would not have been possible. Dr. Mark Hearn and Dr. Qubai Hu have played key role in the process of this study and this work could not be possible without their guidance.

Special thanks to Dr. Daniel Storm, Dr. Raj Kapur, Dr. Lee-Way Jin and Dr. Qubai Hu for serving on my supervising committee. Their critical inputs have significantly improved this dissertation.

Finally, I would like to thank my husband Shenghui Li and my family for their support and encouragement for this endeavor.

To my parents
and
whomever has encouraged me in my life

CHAPTER 1

INTRODUCTION

1.1. Overview

Dementias of the Alzheimer type (DAT) are multi-factorial diseases associated with several genes including the gene (*APP*) for the beta-amyloid precursor protein (βPP). βPP has been thought to be of central importance for the pathogenesis of DAT since the deposition of its proteolytic product, β-amyloid, is found in the main pathological lesion of DAT. Moreover, all three dominant mutations responsible for early onset familial forms of DAT appear to influence βPP processing. The cytoplasmic domain of βPP has been shown to interact with a putative phosphotyrosine interacting domain (PID) of a neural adaptor protein, FE65. FE65 regulates βPP trafficking and processing via strong binding of its PID with the intracellular tail of βPP. In addition to the PID that interacts with βPP, FE65 possesses one more PID domain. The latter interacts with a transcription factor (CP2), with a histone acetyltransferase (Tip60) and with a member of a family of low- density lipoprotein receptor- related protein (LRP). A WW domain (a protein module with two conserved tryptophans) of FE65 interacts with a cytoskeleton associated protein Mena and Abl. Potential functions of FE65 in gene transcription and cytoskeleton remodeling have been studied in vitro.

1.2. Dementias of the Alzheimer type (DAT)

DAT are devastating progressive human neurodegenerative disorders, clinically evidenced by memory loss and cognitive impairments. They are the most common causes of late-life dementias. These disorders debilitate millions of elderly people, affecting up to 5% of those over 65 years and >20% of those over 80 (Launer et al., 1999).

1.2.1. Genetics of DAT

These diseases clearly have complex etiologies. They include early- and late-onset familial forms in addition to much more common "sporadic" forms. Although there are clearly common denominators among these forms, notably canonical elements of the pathways such as beta amyloid deposits and neurofibillary tangles, the possibilities of distinct or partially distinct pathogenic pathways cannot be excluded.

Familial DAT: Familial DAT cases are substantially less frequent than sporadic DAT cases. They are usually associated with the emergence of clinical symptoms earlier than the seventh decade of life. Mutations in at least three genes can lead to autosomal dominantly inherited early onset forms of DAT: the beta amyloid precursor protein gene (*APP*) on chromosone 21 (Goate et al., 1991), the presenilin 1 gene (*PS1*) on chromosome 14 (Sherrington et al., 1995) and the presenilin 2 gene on chromosome 1

(*PS2*) (Levy-Lahad et al., 1995). All the mutations identified in *APP* occur at or near the Aβ encoding sequence, resulting in an enhanced production of the longer, more amyloidogenic Aβ42 peptides (Van Broeckhoven, 1998). All pathogenic mutations in *PS1* and *PS2* are missense mutations suggesting a (toxic) gain of function of the mutated protein. With respect to βPP processing, most presenilin mutations cause an increased secretion of the Aβ 42 and Aβ 43 (Borchelt et al., 1996; Tomita et al., 1997; Citron et al., 1997), suggesting a central role of Aβ in DAT pathogenesis.

Sporadic DAT: An allelic variant (ε4) of the apolipoprotein-E gene (APOE) has been associated with sporadic and familial disease with onset usually after age 65 years. A single APOE-ε4 allele increases the risk of disease ~twofold, whereas the homozygosity causes at least a fivefold increase in risk. These figures vary among different ethnic groups. Aging is the major risk factor for DAT, however.

1.2.2. Pathology of DAT

The neuropathology of DAT is characterized by extensive regional neuronal and synaptic loss, with the presence of neuritic plaques, neurofibrillary tangles and cerebrovascular amyloidosis in the brain. The major components of neuritic plaques are parenchymal deposits of a fibrillar 4-kD protein of 40 to 43 amino acids, beta amyloid (Aβ). These are surrounded by dystrophic neurites. Neurofibrillary tangles are neuronal cytoplasmic aggregates composed of paired helical filaments of hyperphosphorylated tau protein, a microtubule- associated protein. These

histpathological lesions are spatially and temporally restricted. The hippocampus and temporal cortex are particularly affected.

1.2.3. DAT pathogenesis: Amyloid hypothesis

One of the most prominent mechanisms proposed to underlie the neurodegeneration is the accumulation of β-amyloid plagues. This view has been called "Amyloid Cascade Hypothesis". It proposes that accumulations of Aβ (resulting from overproduction, altered processing, or a failure of clearance) is an initiating event in the pathological cascade of events leading to all forms of DAT (reviewed by Selkoe, 2001). By that view, Aβ is not merely a disease marker; it plays a causal role in the development of DAT. The strongest support for this hypothesis came from the observation that all of the genes that are now known to increase susceptibility to DAT (*APP*, *PS1*, *PS2* and *ApoE*) consistently alter Aβ metabolism in a manner likely to enhance Aβ aggregation and amyloid deposition. This hypothesis is supported by numerous *in vivo* and *in vitro* studies showing that Aβ aggregates can directly and indirectly mediate changes in calcium homeostasis, oxidative injury, and inflammatory responses (reviewed by Yankner, 2000). Hyperphosphorylation of tau, which results in neuronal dysfunction and death, is believed by most investigation to be one of a series of downstream neurotoxic events initiated by Aβ accumulation. The cumulative effects of the direct Aβ-induced injury together with secondary injury that is induced by the neurofibrillary tangles are likely to result in neuronal dysfunction and death and synaptic loss, giving rise to the clinical symptoms of dementia.

1.3. The beta-Amyloid Precursor Protein (βPP)

1.3.1. βPP metabolism:

Aβ is derived from the proteolytic processing of a large precursor polypeptide, the [beta]-amyloid precursor protein (βPP) (Kang et al., 1987). βPP is a glycosylated integral membrane protein that contains a large N-terminal ectodomain, a single tran-membrane region and a short cytoplasmic domain. After delivery to the cell surface via a constitutive biosynthetic pathway, βPP is either cleaved by α-secretase, releasing the large soluble extracellular amino-terminal portion of βPP (βPPsα) or re-internalized by endocytosis, resulting in the generation of Aβ (Koo & Squazzo, 1994). α-secretase cleavage occurs within the Aβ sequences and therefore precludes the generation of Aβ (Esch et al., 1990). The resulting carboxy-terminal fragment (CTFα), consisting of 83 residues, can undergo further cleavage by γ- secretase to liberate the P3 peptide, which is believed to be non- amyloidogenic. Two members of the disintegrin metalloproteinase family, tumor necrosis factor-α (TNF-α)-converting enzyme (TACE) and ADAM10 have been shown to be involved in α-secretase activity (Buxbaum et al., 1998; Parvathy et al., 1998; Lammich et al., 1999). The internalization of cell surface βPP occurs is clathrin-mediated and requires the NPXY motif in the cytoplasmic tail of βPP (Haass and Selkoe, 1993; Nordstedt et al., 1993). This internalization pathway can lead to Aβ peptide formation as a consequence of the action of the two proteolytic activities (β- and γ-secretase). These cleave at the amino-

terminus and carboxy-terminus of the peptide, respectively (De Strooper and Annaert, 2000). Cleavage by β-secretase generates a secretary amino terminus (βPPsβ) and the membrane associated amyloidogenic carboxy-terminal fragment (C99; consisting of 99 residues). Further cleavage of C99 by γ- secretase releases Aβ and the βPP intracellular domain (AICD), which is the carboxy-terminal of βPP. Although the majority of Aβ molecules are formed in the endocytic pathway, some Aβ may be produced in the secretary pathway as well (Selkoe, 1996). Whereas the aspartic protease BACE1 (β-site βPP-cleaving enzyme) has been identified as the major β-secretase (Cai et al., 2001), the identity of γ -secretase has remained elusive. Evidence suggests that γ -secretase is a large protein complex consisting of presenilin-1 as the catalytic subunit (Li et al., 2000) and other proteins (perhaps regulatory) such as Nicastrin (Yu et al., 2000; Esler et al., 2002). A novel ε-site cleavage site of βPP distal to the canonical γ-secretase site has been identified recently; it produces an AICD fragment consisting of the last 50 carboxy-terminal residues of the βPP (See Fig 1.1). This ε-site cleavage is presenilin-dependent and is sensitive to γ-secretase inhibition (Yu et al., 2001; Weidemann et al., 2002). The roles of the different γ-secretase mediated cleavage sites in the generation of Aβ are not known.

1.3.2. βPP functions

Although the precise functions of βPP are not clear, several possible roles as a multifunctional protein have been proposed (See review by Mattson, 1997).

1). Cell adhesion and neurite outgrowth. It has been suggested that βPP may play a role in the outgrowth and/or maintenance of axons or nerve terminals. This view was supported by several studies documenting co-localization of βPP with β1 integrins at focal contact sites of differentiating neuronal cells (Yamazaki et al., 1997) and enhancement of neurite outgrowth (Qiu et al., 1995). Evidence for such a role was came from the finding that hippocampal neurons derived from βPP-deficient mice display deficient neuritic branching and outgrowth (Perez et al., 1997).

2). Synaptic plasticity. βPP has a preferential localization at central and peripheral synaptic sites, suggesting that βPP may play a role in synapse formation and maintenance (Sisodia & Gallagher, 1998). Indeed, βPP-null mice have deficits in spatial learning and hippocampal synaptic plasticity (Dawson et al., 1999). These deficits are associated with both pre- and post-synaptic structural changes (Seabrook et al., 1999).

3). Neurotrophic actions of sAPPα. Studies have shown that secreted βPP (sAPPα) fulfills synaptotrophic and neuroprotective functions within the central nervous system (CNS) in response to various stressful conditions, including excitotoxicity (Mattson, 1994) and ischemia (Smithswintosky et al., 1994).

4) Axonal transport. More recent evidence suggests that βPP might be an axonal transport receptor, as it binds to the light chain subunit of kinesin 1, a microtubule motor protein (Kamal et al., 2000).

1.3.3. βPP Binding Proteins:

Recent progress on βPP functions has come from studies of the cytoplasmic protein network interacting with the C-terminal tail of βPP. Since protein-protein interactions are the basis for most of the structural and functional organizations within cells, the unraveling of such protein networks and their precise individual functions could therefore be valuable approaches in the determination of the normal and abnormal physiological function(s) of βPP.

At least three adaptor-like proteins have been found to interact with the C-terminal domain of βPP. One of these is FE65, a neuronal adaptor protein that will be discussed in detail in the next section. A second neuronal adaptor protein is X11 (Borg et al., 1996; McLoughlin et al., 1996), which also binds to the YENPTY motif of βPP, and competes with FE65 for binding to βPP (Lau et al., 2000). Overexpression of X11 retards the processing of βPP, resulting in decreased secretion of sβPP and Aβ in transfected HEK 293 cells (Borg et al., 1998). mDab1 (Mammalian orthologue of *Drosophila* Disabled) is a third adaptor protein shown to interact, via its PID, with the NPXY motif of βPP (Trommsdorff et al., 1998; Homayouni et al., 1999). Thus, at

least three molecular pathways might compete for binding to βPP. Other proteins that interact with the C-terminal of βPP include: a brain specific GTP-binding protein G_0 (Nishimoto et al., 1993, Bruillet et al., 1999). , a cell cycle related protein, βPP-BP1 (Chow et al., 1996; Chen et al., 2000), ShcA (SH2-domain-containing transforming protein 1) (Russo et al., 2002), a microtubule-interacting protein, PAT1 (Protein interacting with APP tail 1) (Zheng et al., 1998), nicastrin (Yu et al., 2000) and Kinesin-1 light chain subunit (KLC) (Kamal et al., 2000), Jip 1(JNK-interacting protein) (Matsuda et al., 2001; Scheinfeld et al., 2001), Abl tyrosine kinase (Zambrano et al., 2001), and adaptor protein Shc (Tarr et al., 2002). Functional balances among these proteins might be important for the regulation of βPP metabolism and function (De Strooper, 2000).

1.4. FE65- An Adaptor Protein:

Adaptor proteins are defined as proteins that augment cellular responses by recruiting other proteins to a complex. Adaptor proteins usually contain several protein-protein-interaction domains. FE65 meets these definitional criteria as it brings together multiple proteins via its protein interacting domains to form a complex surrounding βPP.

1.4.1. FE65 Domain Structures and Binding Proteins

Yeast two hybrid system screens for proteins interacting with βPP resulted in the identification of an interaction between the cytoplasmic tail of βPP and FE65p. (Fiore

et al., 1995; Bressler et al., 1996). The *FE65* gene was originally identified in a screen for neural specific transcripts (Duilio et al., 1991). Sequence analysis has shown that FE65, a 710 amino acid protein, contains three different consensus protein interaction domains- two phosphotyrosine interacting domains (PID) and a WW domain (Bork and Sudol 1994; Bork and Margolis 1995). It is the C-terminal PID (PID2) that interacts with the C-terminal domain of βPP in a region surrounding the YENPTY motif (Fiore et al., 1995; Bressler et al., 1996; Borg et al., 1996). While previously described PID domains bind to phosphorylated binding sequences, there is no evidence that phosphorylation of the YENPXY sequence within the cytoplasmic domain of βPP is required for FE65 (Borg et al., 1996). PTB domains bind the consensus sequence NPXY, which is present in the cytoplasmic domains of several cell-surface receptors, including the epidermal growth factor receptor (Blaikie et al., 1994), the insulin receptor (He et al., 1995), nerve growth factor receptor (TrKA) (Obermeier et al., 1994), and the LDL receptor (Davis et al., 1986).

The FE65 PID 1 domain binds to the CP2/LSF/LBP1 transcription factor (Zambrano et al., 1998). FE65 has been found to form complexes with CP2/LSF/LBP1. These complexes are present in cytoplasm and nucleus. Another strong interactor of FE65 PID1 is histone acetyltransferase Tip60 (Cao and Sudhof, 2001). Therefore, FE65 may be involved in several nuclear processes via its PID1 domain. In addition to CP2 and Tip 60, the PID1 of FE65 also has been found to interact with LRP (Low density

lipoprotein receptor-related protein) (Trommsdorff et al., 1998), a neuronal surface receptor that binds and internalizes apolipoprotein E, βPPs and a2-macroglobulin.

The WW domain is the most N-terminal of the three FE65 protein interacting domains. It is a small module composed of 40 amino acids with two signature tryptophan (W) residues spaced 20-22 amino acid apart (Sudol et al., 2001). Many proteins with WW domains have been found in the nucleus and have been documented to participate the modulation of RNA polymerase II activity (reviewed by Sudol et al., 2001). The WW domain of FE65 has been demonstrated to interact with Mena (Mammalian homologue of Drosophila enabled protein), EVL (Ena-VASP like) and other unidentified proteins (Ermekova et al., 1997; Lambrechts et al., 2000). Mena and EVL belong to a family of Ena-related proteins including *Drosophila* Ena (Enabled) and VSAP (vasodilator-stimulated phosphoprotein) (Gertler et al., 1996). All members of the Ena/VASP family share common sequence motifs consisting of an amino-terminal Ena-VASP-homology (EVH1) domain, a central proline-rich domain, and a carboxy-terminal EVH2 domain (See review by Lanier and Gertler, 2000). The WW domain of FE65 binds to the central proline-rich sequence of Mena. This region of Mena also binds to the actin monomer-binding protein profilin and to other proteins with SH3 domains including Abl. The EVH1 domain targets family members to focal adhesions while the EVH2 domain binds to F-actin. Mena and the Ena/VASP family are involved in microfilament assembly and cell motility (Laurent et al., 1999). They are found in areas of dynamic actin remodeling such as axonal growth cones (Gertler

et al., 1996). In mice, deletion of Mena causes defects in the formation of the corpus callosum and the hippocampal commissure, suggesting that Mena plays a role in growth cone motility and/or axon guidance (Lanier et al., 1999). In addition to Mena, WW domain of FE65 was found to interact with the Abl non-receptor tyrosine kinase (Zambrano et al., 2001). Therefore, FE65 is likely to act as a bridging molecule between βPP and Abl for tyrosine kinase- mediated signaling.

1.4.2. The FE65 family

FE65 is a member of a multigene family. In mammals, identified member are the human FE65-like (FE65 L1) (Guenette et al. 1996), rat FE65 L2 (Duilio et al., 1998) and human FE65 L2 (Tanahashi et al., 1999). They all share certain highly conserved domains with FE65 with, and therefore also have the characteristics of adaptor proteins. They have been shown to bind the NPXY motif of the cytosolic domain of βPP through their PID2 domains (Guenette et al. 1996; Duilio et al., 1998; Tanahashi et al., 1999). FE65 L1 and L2 were found in the nucleus and cytosol (Bruni et al., 2002; Tanahashi et al., 2002). All of them have been shown to be able to block cell cycle progression (Bruni et al., 2002). However FE65 L2 has poor ability for transactivation, suggesting that FE65 L2 has a different nuclear function from FE65 (Tanahashi et al., 2002). Both FE65 L1 and FE65 L2 have been shown to increase the secretion of Aβ when overexpressed in cell culture (Guenette et al., 1999; Tanahashi et al., 2002). The tissue distribution patterns for the three proteins are also distinct. In contrast to FE65, which is predominantly expressed in brain, FE65 L1 is ubiquitously

expressed and FE65 L2 is equally expressed in brain and testis, with low levels in other tissues (Guenette et al. 1996; Duilio et al., 1998). Two isoforms of human FE65 L2, resulted from alternative splicing of the RNA, do not contain the PID2 domain and therefore do not bind βPP (Tanahashi et al., 2002). These two isoforms are exclusively localized to nucleus (Tanahashi et al., 2002).

1.4.3. FE65 Functions

1. Regulating βPP processing. Since the YENPTY motif mediates the internalization of βPP and is required for subsequent Aβ formation (Koo and Squazzo, 1994; LeBlance and Gambetti, 1994), interactions between βPP and FE65 can potentially affect proteolytic processing of βPP into the neurotoxic Aβ peptide. Indeed, over-expression of *FE65* in Madin-Darby canine kidney cells increased translocation of βPP to the cell surface, and increased both sβPPα and secreted Aβ (Sabo et al., 1999). An opposite effect of FE65 on Aβ production has also been reported, however (Ando et al., 2001).

2. Cell movement. Given the fact that FE65 interacts with the Mena protein, FE65 is likely to be involved in cytoskeleton remodeling events, such as cell adhesion, neurite extension or synaptic remodeling. Sabo et al., have shown that FE65 and βPP synergistically regulate actin-based membrane motility in transfected cells and in neurons (Sabo et al., 2001 and 2003).

3. Gene transcription. FE65 appears to have an important role(s) in nuclear processes. FE65 was found both in the cytoplasm and in the nucleus (Zambrano et al., 1998). The region responsible for FE65 nuclear targeting has been mapped to the N-terminal of FE65 in a region containing about 100 amino acids, including the WW domain (Minopoli et al., 2001). Phosphorylation of FE65 at the potential phosphorylation sites 5' of the WW domain might be required for FE65p cytosol-nuclear translocation (Zambrano et al., 1998). Given the evidence that it has a nuclear localization signal and contains a putative DNA binding domain (Duilio et al., 1991), FE65 may function as a transcriptional activator. Recently, FE65 has been found to form a transcriptionally active complex with the AICD of βPP and Tip60 (Cao and Sudhof. 2001). All the protein interacting domains of FE65 seem to be required for this transcriptional activity (Cao and Sudhof. 2001).

1.4.4. The Role of FE65 in DAT

FE65 was found to be abundantly expressed in neurons. The areas of highest expression included regions of the hippocampus, the structure in which the earliest DAT pathology are detectable. Two independent studies have shown that genetic polymorphisms in the *FE65* gene are associated with a reduced risk of sporadic DAT. These observations have biological plausibility based upon altered interactions of the FE65 allelic variants with βPP (Hu et al., 1998; Lambert et al 2000; Hu et al., 2002). Two studies, however, have failed to find such associations (Papassotiropoulos et al.,

2000; Guenette et al., 2000). The current interpretation of these conflictive results is that the polymorphic association is most readily detected in DAT patients over the age of 75 years. Recently, a c954C→T polymorphism in the FE65 L2 gene was found to be associated with early-onset DAT (Tanahashi et al., 2002b). Altered expression of *FE65* mRNAs in DAT brains has also been found (Hu et al., 2000). Finally, increased FE65 immunoreactivity in hippocampal area CA4 of very late- onset DAT brains might be associated with the increased severity of the disease (Delatour et al., 2001). All these lines of evidence suggest that FE65 could be involved in the pathogenesis of certain forms DAT.

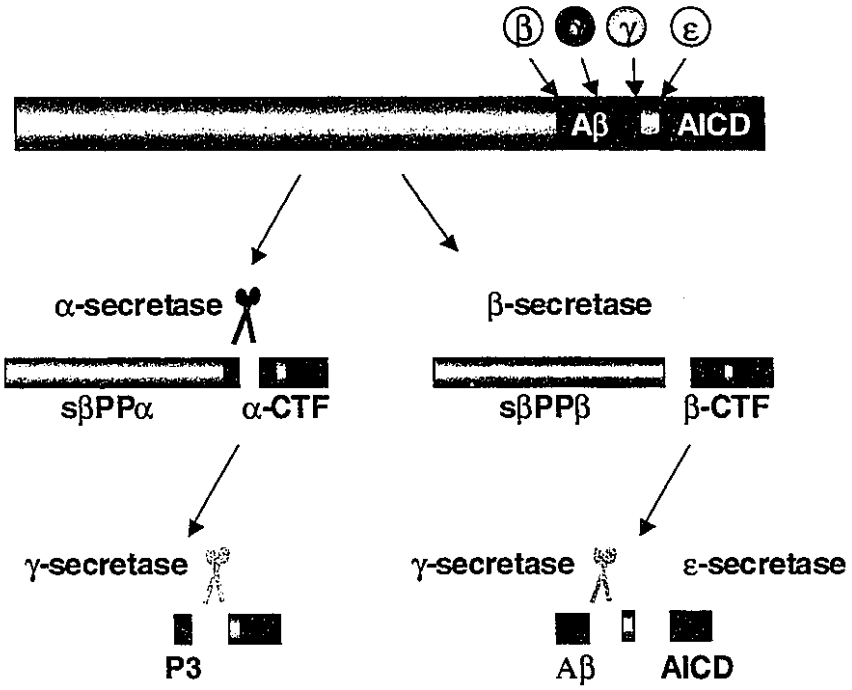

Figure 1.1. Proteolysis of βPP.

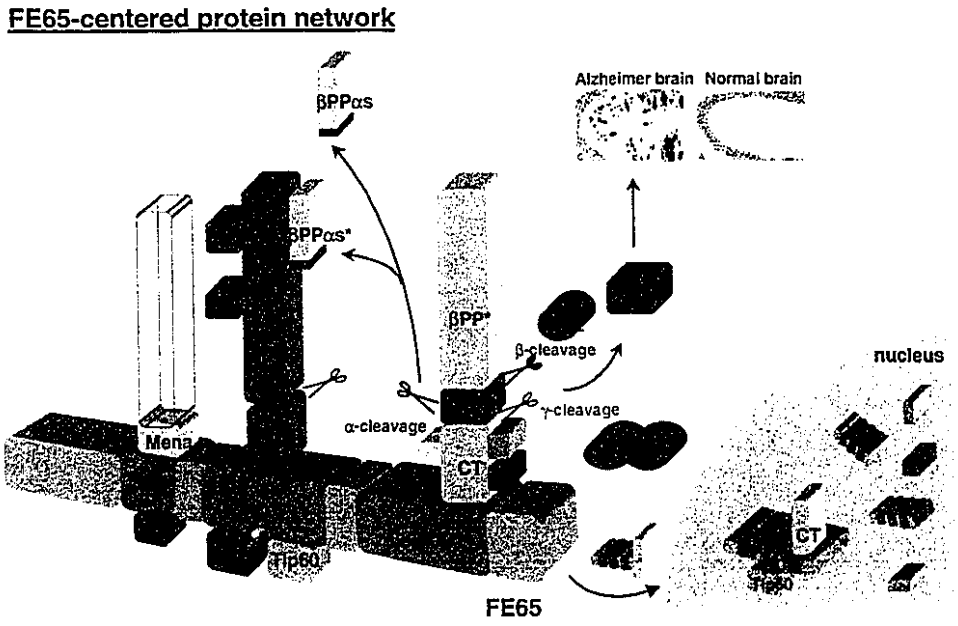

Figure 1.2. The FE65 centered interacting protein network. Asterisks indicate genes in which DAT-related mutations and/or polymorphisms have been reported. C: C-terminus; N: N-terminus. Arrows indicate interacting protein domains. Only a limited number of known interactions are illustrated. The choice of cerebellar cortex to illustrate diffuse beta amyloid depositions was motivated by evidence that in these presumably early stages of DAT, FE65 isoforms have been shown to be up-regulated (Hu et al., 2000).

CHAPTER 2

GENERATION AND CHARACTERIZATION OF ISOFORM SPECIFIC FE65 KNOCKOUT MICE

2.1. Introduction

The *FE65* gene was originally identified in a screen for neural specific transcripts (Duilio et al., 1991). Its full-length neuronal form contains 710 amino acids with apparent molecular mass of ~97 kDa. Because FE65 possesses three protein-protein interacting domains, a WW domain followed by two PIDs, it is capable of forming complex protein networks (Russo et al., 1998). In addition to binding to the βPP intracellular domain (AICD), the more N-terminal PID interacts with the transcription factor CP2/LSF/LBP1 (Zambrano et al., 1998), histone acetyltransferase Tip60 (Cao and Südhof, 2001) and a member of the low-density lipoprotein receptor-related protein family, LRP1 (Trommsdorff et al., 1998). The WW domain, located at the N-terminus of FE65, interacts with Mena (the mammalian homologue of the Drosophila *enabled*) (Ermekova et al., 1997) and Abl, a non-receptor tyrosine kinase (Zambrano et al., 2001). FE65 is found in both cytoplasm and nucleus at subcellular levels (Zambrano et al., 1998; Minopoli et al., 2001). *In vitro* studies implicated roles of FE65 in the metabolism of βPP (Sabo et al., 1999; Guenette et al., 1999), cell

movement (Sabo et al., 2001), transcriptional activation (Cao and Südhof, 2001; Baek et al., 2002) and cell cycle regulation (Bruni et al., 2002).

βPP is widely accepted as a central player in the pathogenesis of dementias of the Alzheimer type, of which a major feature is memory loss (for recent reviews, see Selkoe 2001 and 2002). βPP is among a number of proteins whose processing is regulated by presenilin-dependent regulated intramembrane proteolysis (RIP) (Brown et al., 2000). α-cleavage of βPP generates a soluble βPP ectodomain and a membrane-associated C-terminal fragment; β-and γ-cleavages of βPP also release a monomeric Aβ and AICD. This process resembles Notch nuclear signaling (Annaert and De Strooper 1999; Brown et al. 2000). Recent evidence suggests that FE65 may play a critical role in the assembly of multimolecular signalling complexes, including AICD and Tip60, for propagation of signals from extracellular and cytoplasmic domains to the nucleus (Cao and Südhof, 2001; Baek et al., 2002).

In order to better define the physiological role of FE65 *in vivo*, we have generated a mouse strain carrying a disrupted *FE65* locus via homologous recombination. A detailed molecular and physical characterization of these mice will be described in this chapter.

2.2. Materials and Methods

2.2.1. Determination of the Mouse FE65 cDNA Sequence

Partial mouse cDNA sequences were obtained from the Genbank database by "electronic hybridization" with the human *FE65* sequence (Bressler et al., 1996; Hu et al., 1998). The remainder of the mouse *FE65* cDNA sequence was determined using standard sequencing protocols (Sanger et al., 1977). The 5' terminus of mouse *FE65* cDNA was determined by 5' RACE reactions with total RNA isolated from mouse brain tissues. Mouse *FE65* sequences are 89% identical at the nucleic acid level and 95% identical at the amino acid level, as compared to the human *FE65* sequences (Fig. 2.1). The full-length coding sequence of mouse *FE65* was cloned into the expression vector pCAGGS described by Niwa et al. (1991).

2.2.2. Construction of a FE65 Gene Targeting Vector

To obtain the mouse *FE65* genomic DNA, approximately 1×10^6 phage plaques of a C57/BL6 mouse genomic DNA library (Lambda DASH II, Stratagene, La Jolla, CA) were screened with a cDNA probe containing exons 11-13 of the mouse *FE65* cDNA (Bressler et al., 1996). Eleven overlapping genomic clones were isolated. The longest one, containing part of intron 1 (6 kb) through exon 12 (15 kb total, see Fig 2.3), was subcloned into a NotI site of a pBlueScript vector (Stratagene, La Jolla, CA), and used to construct a targeting vector. The procedure involved in generating gene-targeted mice is shown in Fig 2.2. To construct the targeting vector, a 2.8 kb HindIII/BstBI fragment including part of intron 1 and 164 bp of 5' exon 2, and a 5.5 kb NheI

fragment containing 106 bp of 3' exon 2 and part of intron 2 were inserted into the ClaI, and the SpeI sites, respectively, of a pNTK2 gene targeting vector (Zhou et al., 1995; see Fig 2.4). The resulting construct (Fig. 2.4) has two herpes simplex thymidine kinase (TK) genes at both ends of the homologous sequence, and a phosphoglycerate kinase (PGK) promoter-driven neomycin cassette (Neo), which replaced most of the exon 2 region of the *FE65* gene.

2.2.3. Selection of Homologous Recombinant ES Cell Clones and Production of Mutant Mice

129/Sv derived R1 embryonic stem (ES) cells (Nagy et al., 1993) were cultured on γ-irradiated primary mouse embryonic fibroblast feeder cells in Dulbecco's modified Eagle's medium (DMEM; Gibco-BRL, Gaithersberg, MD) supplemented with 15% heat-inactivated fetal bovine serum (FBS; HyClone, Logan, UT), 2mM glutamine, 0.1 mM MEM nonessential amino acids, 1mM MEM sodium pyruvate solution, 0.1 mM β-mercaptoethanol, and 1000 U/ml murine leukemia inhibitory factor (Gibco-BRL, Gaithersberg, MD). The cells were cultured in an atmosphere of 5% CO2 in air in a humidified incubator at 37%. pNTK2-*FE65* DNA (10-20 μg) was linearized by digestion with a SacI restriction enzyme and transfected into 1×10^7 ES cells by electroporation under the conditions of 800 V and 25 μF capacitance, using the Bio-Rad Gene Pulser apparatus (Bio-Rad, Hercules, CA). The cells were then plated onto 100 mm plates. 200 μg/ml of G418 (Geneticin; Gibco-BRL, Gaithersberg, MD) and 2 μM of gancyclovir (Roche, Palo Alto, CA) were applied 48 h later. Doubly resistant

colonies were picked after 8-10 days and analyzed by polymerase chain reaction (PCR) analysis and Southern blotting for homologous recombination events (Fig. 2.5). Six out of 51 ES clones showed the expected homologous recombination. The euploidy of these clonal ES cell lines was confirmed by cytogenetic examination as previously described (Martin et al., 1985). Two independently targeted ES cell clones were injected into 3.5-d.p.c.C57B/6 blastocysts, and transferred to pseudopregnant females to produce male chimeric mice. The contribution of these stem cells to the germline of chimeric mice was assessed by breeding with C57BL/6 females and by screening for agouti offspring. Germline transmission of the FE65 mutation was achieved with both of the injected ES cell lines. F1 heterozygous animals were back-crossed to C57BL/6 mice to maintain the disrupted allele. Mice heterozygous for the FE65 mutation were intercrossed to generate homozygous mutant knockout mice. Genotyping was carried out by PCR analysis (Fig. 2.5) with two forward primers, M230-5 (5'-GCCCACAATGCAGCCAACCGAGG, wild type *FE65*-specific) and NEO-4 (5'-CGCCTTCTTGACGAGTTC, mutant *FE65*-specific), and a reverse primer M230-48 (5'-CTGTGTCCTCCGGGGAGCCATGG).

2.2.4. Northern Analysis and RT-PCR

Approximately 20 of ug RNA of each sample was used for Northern analysis (Bressler et al., 1996). Blots were hybridized with FE65 cDNA probes indicated in Fig, 2.6. The stripped blot was then hybridized with a β-actin cDNA probe for normalization of loading samples. Reverse transcription (RT) was carried out using

reverse transcriptase (GibcoBRL, Gaithersburg, MD) with random hexamers. Total RNA (2ug) was reverse transcribed. Single strand cDNA was subjected to PCR amplification with primers specific to FE65 exons as described in Fig. 2.4.

2.2.5. Western Analysis

Affinity-purified rabbit polyclonal antibodies against different epitopes of FE65 protein were used (Hu et al., 2002). Antibody FE27 recognizes an N-terminal epitope of FE65 (amino acids 27 - 36: PLHAAHNQLL), immediately downstream of the first AUG codon in the open reading frame (ORF) of *FE65*. Antibody FE518 recognizes a C-terminal epitope (amino acids 518 - 527: LDHSKLVDVP) between the PID1 and PID2. All the epitope sequences are conserved between human and mouse; none of them have homology with other family members, FE65 L1 and FE65 L2. Anti-βPP C-terminal antibody (B994) has been described previously (Jin et al., 1998). The following commercially available antibodies were also used: anti-c-abl (Oncogene Research Product, San Diego, CA), anti-Tip60 and anti-X11α (Santa Cruz Biotechnology, Santa Cruz, CA), anti-LRP (Research Diagnostics, Flanders, NJ), 22C11 (Chemicon, Temecula, CA), Anti-βPP C-terminal antibody (Sigma, St Louis, MO), anti-Mena and anti-CP2 (BD Transduction Laboratories, Lexington, KY).

Whole mouse brains were dissected on ice and homogenized at 100 mg/ml in a cold lysis buffer (50 mM Tris HCL, ph 7.4, 150mM Nacl, 0.5% Triton-X100, 10% glycerol, 50mM NaF, 1mM sodium vanadate) supplemented with protease inhibitor

cocktail, Complete EDTA-free™ (Roche, Palo Alto, CA). Brain lysates were subjected to electrophoretic separation on 7.5% SDS-polyacrylamide gels (SDS-PAGE). Western analysis was performed as previously described (Hu et al., 2002).

2.2.6. Histopathological Studies

Mice were euthanized using carbon dioxide gas. The calvarium was carefully removed while leaving the brain intact and, along with thoracic and abdominal organs, the entire caracass was placed in 10% neutral phosphate buffered formalin for fixation. Following fixation for several days sections of brain were prepared using a rodent brain matrix (Electron Microscopy Sciences, Ft. Washington, PA). Coronal sections of brain were taken approximately every 2 mm. These sections, along with those of other tissues, were embedded in paraffin and stained with H&E. Tissues were examined by a murine pathologist (Dr. Dennis H. Liggit); he was unaware of the genotypes.

2.2.7. Neuronal Cultures

Primary cortical neuron cultures from ~2-48 hour newborn mice were prepared as described by Xiang et al (1996). Briefly, cells were initially dissociated by trypsinization (0.25% in Hanks' Balanced Salt Solution, Ca^{2+} - and Mg^{2-} -free; GibcoBRL, Gaithersburg, MD) for 25 min at 37°C, and were further dissociated in serum-free Neurobasal medium supplemented with B27 (Life Technologies, Gaithersburg, MD). Cells were then plated on poly-D-lysine-coated dishes (1 ug/ml) at

2×10^6 cells per 60 mm dish in Neurobasal/B27 medium. This medium has been reported to support long-term survival (several weeks) of cultures of newborn neurons while suppressing glial growth to < 2% of the total cell population (Xiang et al., 1996).

2.2.8. Aβ Quantitation

Aβ peptides in conditioned medium of primary neuronal cultures were quantified by electrophoresis in Bicine-urea PAGE followed by immunoblotting as described by Klafki et al. (1996) and Wiltfang et al. (1997). Ten ul of conditioned culture media were loaded and separated on a 16.5% mini bicine-urea PAGE gel at 100 volts for 2 hours. Proteins were transferred to an immobilin-P membrane (Millipore, Watertown, MA) by a semi-dry electrophoretic transfer cell (Bio-Rad, Hercules, CA). Membranes were boiled in phosphate-buffered saline for 3 min and immunoblotted with a mouse monoclonal antibody 6E10 (Signet, Dedham, MA). Exposed films were scanned with an AGFA scanner (ARCUSII, Taiwan) using Adobe PhotoShop (Adobe, San Jose, CA). Intensities of protein bands on scanned images were quantitated using Scion Image software (Scion Corporation, Frederick, MD). Authentic Aβ 40 and Aβ 42 peptides (Quality Controlled Biochemicals, Hopkinton, MA) were used as internal standards for the identification of the corresponding Aβ species in the gel preparations.

2.3. Results

2.3.1. Molecular Characterization of FE65 Mutant Mice

To create a mutation in the *FE65* gene, we targeted its exon 2 (the first coding exon) in ES cells. Exon 2 is the largest exon; it encodes 245 amino acids (one third of FE65 protein), including the first three ATG translational start sites.

2.3.1.1 Northern analysis and RT-PCR

Levels of *FE65* mRNA in brain tissues of knockout mice were determined by Northern analysis and RT-PCR. In Northern analysis, two different *FE65* DNA fragments were used as probes for hybridization, a 680 bp fragment corresponding to exon 2 and a 626 bp fragment corresponding to exon 11-14. Both probes hybridized with 2.6 kb mRNA bands, the expected results for wild type *FE65* mRNA. In contrast, the 2.6 kb *FE65* mRNA was not detected in *FE65* knockout mice (Fig. 2.6), indicating that expression of the full-length *FE65* mRNA was interrupted in these mice. The intensities of these bands in heterozygous mice were decreased by 50% when compared with those from wild type mice, after normalization to levels of β-actin mRNA. RT-PCR assays with different pairs of primers were conducted to determine whether *FE65* transcripts were completely absent in *FE65* knockout mice. Using a forward primer 5' to the neo insertion (in exon 1, see Fig. 2.2) in combination with a reverse primer 3' to the insertion (in exon 3) for PCR assays, we detected 937 bp cDNA bands in wild type mouse brain RNA, as expected, and a shorter, circa 700 bp cDNA band in RNA samples from *FE65* knockout mouse brains (Fig. 2.6). DNA

sequencing of the shortened PCR product revealed that it was a *FE65* transcript with a precise excision of exon 2. These data suggested that the targeted exon from the *FE65* knockout mice had sometimes been skipped during splicing, giving rise to mRNA transcripts lacking 735 bp of exon 2. Since all three potential ATG start codons are in the exon 2, the transcripts with skipped exon 2 may not be functional.

2.3.1.2 Western Analysis and GST-βPP-C48 Pull Down Assays

Western blot analysis with antibodies specific to the N-terminus (FE27) or to the C-terminus (FE518) of FE65 confirmed absent expression of the 97 KDa full-length FE65 in the brain lysates of homozygous mutant mice, and reduced expression in heterozygous animals, reflecting a gene-dosage effect of the mutation (Fig 2.7). Since FE65 protein has a high binding affinity for the C-terminus of βPP, GST-βPP-C48 pull-down assays were performed to confirm the western results. The results revealed that both the N-terminal and C-terminal FE65 antibodies recognized full-length FE65 proteins as a 97 kD band. This band was found in brain lysates from wild type mice but not in lysates from *FE65* knock out mice (Fig. 2.7), indicating that full-length FE65 proteins are not expressed in $FE65^{-/-}$ mice. However, antibody FE518 (the C-terminal FE65 antibody) also recognized novel 60 kD bands in brain lysates from both wild type and *FE65* knockout mice. The densities of the 60kD bands appeared to be stronger in brain lysates from $FE65^{-/-}$ mice as compared with those from $FE65^{+/+}$ mice. To further characterize the 60 kDa bands, an additional FE65 antibody, FE352, whose epitope is localized at the beginning of the PID1 sequence, was used. Although FE352

antibody is not strong enough for the detection of proteins in direct Western analysis (data not shown), it could easily recognize both 97 kDa and 60 kDa FE65 proteins in pull-down materials (Fig. 3.1). Because none of these epitopes have homologous residues with the other FE65 family members, we conclude that the 60 kDa fragment is derived from the same ORF of the *FE65* gene. We therefore refer to the 97 kDa full-length FE65 protein (710 amino acids), initiated from the first ATG codon, as p97, and the 60 kDa protein as p60. p60 is an alternatively initiated form of FE65 protein, which is normally present in wild type mice at low levels and is significantly upregulated in our *FE65* mutant mice. Levels of p60 in the brain lysates of *FE65* mutant mice were increased about 5-fold when compared to those of wild type mice (Fig. 2.7; Fig. 3.1). The increased expression may be a compensatory response to the loss of p97 functions. Alternatively, it may be result from the deletion of the first ATG codon in the mutant mice, which normally would suppress protein translation from an internal ATG codon (Kozak 2002). A description of the characterization of the 60 kDa protein is in the next chapter.

2.3.1.3. Evidence for Normal Expressions of FE65 L1/L2

It is possible that overexpression of FE65 L1 and/or FE65 L2 might compensate, or partially compensate, for lost FE65 functions in our *FE65* knockout mice. Therefore, we quantitated levels of *FE65 L1* and *FE65 L2* mRNAs in brain tissues of 6 month-old mice by Northern analysis. Our results showed that levels of the two mRNAs were not significantly changed among $FE65^{+/+}$, $FE65^{+/-}$ and $FE65^{-/-}$ mice after

normalization to levels of β-actin mRNA (data not shown). We could not rule out, however, compensatory alterations in post-transcriptional processes.

2.3.1.4. Evidence for Normal Expressions of FE65-Binding Proteins.

To examine the expressions of known FE65 binding proteins in the brains of p97FE65 knockout mice, western analyses were performed using various antibodies against bPP, mena, LRP, CP2, Tip60, and cAbl. We also assayed the levels of X11α proteins by western analysis. No significant changes were observed for the proteins analyzed when compared to levels in wild type mice (Fig. 2.8).

2.3.2. Physical Characterization of FE65 Mutant Mice

2.3.2.1. General Characterization

The *FE65*$^{+/-}$ and *FE65*$^{-/-}$ mice were viable, fertile, normal in size and appeared healthy, at least up to 36 months of age. Crosses of *FE65*$^{+/-}$ mice resulted in approximate mendelian ratios of progeny. Body weights did not vary among the genotypes. Home cage behaviors, including gait and general activities, were also comparable.

2.3.2.2. Normal Anatomy

Necropsies at 6, 12 and 24 months did not reveal detectible gross abnormalities related to *FE65* genotypes. Detailed histopathological examinations of various tissues of the *FE65*$^{-/-}$ mice at these ages found no abnormalities. Despite the fact that FE65 is widely

expressed in many brain structures, H & E stained coronal sections of mutant mice brains did not show morphological abnormalities.

2.3.2.3. Normal lifespan

A preliminary analysis of the life spans of *FE65*$^{+/-}$ and *FE65*$^{-/-}$ mice revealed no differences as compared to *FE65*$^{+/+}$ (data not shown).

2.3.2.4. Decreased fertilities

During breeding of *FE65* knockout mice, we observed that both female and male *FE65*$^{-/-}$ mice appeared to have decreased fertility, as revealed by reduced litter size and decreased survival of litters. This phenomenon seemed to be more obvious for aged *FE65*-deficient mice as compared to aged wild type control mice.

2.3.3. Crosses of *FE65* mutant mice with Tg2576 mice

In order to study the effects of FE65 on βPP metabolism, we crossed p97FE65$^{+/-}$ mice to Tg(HuAPP695.SWE)2576 mice (Hsiao et al., 1996). This mouse model of DAT expresses human APP_{695} with the 'Swedish' mutation (K670N and M671L) under control of the hamster prion protein (PrP) promoter. Tg2576 mice are well suited for investigating modulation of βPP processing in vivo, because brain Aβ levels are nearly 10-fold above normal endogenous levels, thereby reducing the stringency for assays to detect Aβ, particularly for the less abundant but more amyloidogenic 42-residue form. Tg2576 mice express 5 times more transgene-encoded than endogenous

βPP and develop amyloid plaques by 1 year (Hsiao et al., 1996). Impaired synaptic plasticity and learning have also been found in aged Tg2576 transgenic mice (Chapman et al., 1999). Four female *FE65*$^{+/-}$ mice were initially crossed to 2 male Tg2576 mice. Male Tg2576 mice heterozygous for *FE65* were crossed to female heterozygous *FE65* mice to produce Tg2576 mice that are wild type, heterozygous and homozygous for *FE65*.

2.3.3.1. Decreased Survival Rates for Tg2576 X FE65 F1 Hybrid Mice.

To our surprise, most of our Tg2576/*FE65*$^{-/-}$ mice died prematurely. As shown in Figure 2.9, Tg2576 mice homozygous deficient for *FE65* have reduced survivals as compared with littermate controls (Tg2576/ *FE65*$^{+/+}$). The effect is much more severe in male mice. So far, none of the male Tg2576/*FE65*$^{-/-}$ mice survived beyond 4 months, while a few female Tg2576/*FE65*$^{-/-}$ mice are still alive at 9 months old. Further, Tg2576/*FE65*$^{-/-}$ mice are smaller than littermate Tg2576/*FE65*$^{+/+}$ and Tg2576/*FE65*$^{+/-}$ mice by about 10-20%. This phenomenon is most obvious in males. It is apparent that knocking out the *FE65* gene has a debilitating effect in Tg2576 mice. Deficiency of *FE65* may heighten the toxic effects of *APP* overexpression by altering βPP processing and Aβ deposition or by altering the host response to Aβ neurotoxicity.

2.3.3.2. Reduced Generation of Aβ Peptides in Primary Neuronal Cultures of Tg2576 X FE65 F1 Hybrid Mice

We first assayed the levels of transgene-encoded βPP in the primary neurons of p97FE65$^{-/-}$/Tg2576mice by western analysis. No significant changes were observed compared to those of p97FE65$^{+/+}$/Tg2576 mice (data not shown). Using the bicine-PAGE separation followed by Western analysis method (Klafki et al., 1996; Wiltfang et al., 1997), we observed a linear dose-dependent detection of Aβ peptides. This measurement was quantitative at concentrations of Aβ peptides between 100-800 pg/ lane (20μl) based on our standard curve (Fig. 2.10). Using this assay, we found that the levels of Aβ40 and Aβ42 peptides in conditioned media of primary neuronal cultures from p97FE65$^{-/-}$/Tg2576 mice decreased by 58% ($p<0.02$) and 68% ($p<0.005$), respectively, when compared with those of p97FE65$^{+/+}$/Tg2576 mice (Fig. 2.10). Levels of Aβ40 and Aβ42 peptides from p97FE65$^{+/-}$/Tg2576 mice were also decreased (Fig. 2.10). Values were normalized to levels of the holo-βPP; therefore, the observed differences were not attributable to variations in total βPP levels.

2.4. Discussion

We generated a line of *FE65* mutant mice by homologous recombinational targeting of exon 2 of *FE65*, a multimodulor adaptor or "scaffold" protein (Russo et al., 1998).

We did not achieve our original goal of completely abolishing expression of *FE65* because the disrupted exon was skipped during splicing, resulting in the generation of a shorter read-through transcript. As a consequence, while the mutant mice did not express the full-length FE65 protein (p97), they did express substantial levels of a novel N-terminally-truncated FE65 isoform, p60 (see the next chapter for a detailed description of p60).

Despite the apparent involvement of FE65 in developmental processes (Simeone et al., 1994), we did not observe any developmental deficits. The brain structures, including the hippocampus and cerebellum, regions expressing abundant FE65, were normal by gross and light microscopic examinations. These results suggest that intact FE65 function may not be essential for the normal development of the brain. Alternatively, normal development may be protected via redundant functions of other FE65 family members, such as FE65L1 and FE65L2. Some protection might also be provided by the up-regulated p60.

An interesting, but puzzling, finding of these studies is the altered secretion of neurotoxic Aβ peptides from cultures of primary neurons of Tg2576/*FE65* hybrid mice. Given the fact that p60, which has an intact βPP binding domain, is preserved in the FE65 mutant mice, it seemed unlikely that βPP processing could be altered in these mice. Further studies indicated, however, that although both p60 and p97 have the same binding domain for βPP, their binding affinities to βPP are dramatically

different. p60 has a significantly increased binding affinity to βPP than p97, as shown in the next chapter. Moreover, the two isoforms have distinct subcellular localizations (see the next chapter). These properties of p60 may affect βPP cellular trafficking and the amount of βPP subjected to enzymatic cleavage, resulting in altered levels of cleavage products. These observations indicate important roles of both the N-terminal and C-terminal region of FE65 in the metabolism of βPP.

The premature deaths of Tg2576/FE65-/- mutant hybrid mice made the further analysis of the DAT pathology in these mice difficult. The cause of death is not clear, and might be related in part to the introduction of the C56BL/6 gene from the FE65 line into the Tg2576 genetic background. Increased mortality rates of the Tg2576 mice outbred to C57BL/6 have been report (Carlson et al., 1997). The use of alternated genetic background may permit longer survival and the possibility of detailed histopathological examination.

```
      1                                                                   70
MFE65 GCCDGEAAVL REPCSLSYLR HLGLGPRRAG STKAMSVPSS LSQSAINANS HGGPALSFPL [illegible]
RFE65 ~~~~~~~~~~ ~~~~~~~~~~ ~~~~~~~~~~ ~~~~~~~VRL *AQKGNNANS HGGPALSFPF [illegible]
HFE65 GCCDGEAAAE PEPRSLSHLR HLGPGPHRAG AAKAMSVPSS LSQSAINANS HGGPALSLPL [illegible]
      71                                                                 140
MFE65 NAKLQATAVV PKDLRSAMGE GSVPEPGPAN AKWLKEGQNQ LRRAATAHRD QNRNVTLTLA EEASQEAETA
RFE65 NAKLQATAVV PKDLRSAMGE GSVPEPGPAN AKWLKEGQNQ LRRAATAHRD QNRNVTLTLA EEASQEAETA
HFE65 NAKLQATAVG PKDLRSAMGE GGGPEPGPAN AKWLKEGQNQ LRRAATAHRD QNRNVTLTLA EEASQEPEMA
      141                                                                210
MFE65 PLGPKGLMHL YSELELSAHN AANRGLHGSA LIINTQEQGP DEGEEKAAGE AEEDDEDEEE E.EEEEDLSS
RFE65 PLGPKGLMHL YSELELSAHN AANRGLHGSA KIINTQGLGP DEGEEKAAGE VEEEDEDEEE EDEEEEDLSS
HFE65 PLGPKGLIHL YSELELSAHN AANRGLRGPG LIISTQEQGP DEGEEKAAGE AEEEEEDDDD E.EEEEDLSS
      211                                                                280
MFE65 PPGLPEPLEN VEVPSGPQAL TDGPREHSKS ASLLFGMRNS AASDEDSSWA TLSQGSPSYG SPEDTDSFWN
RFE65 PQGLPEPLEN VEVPSGPQVL TDGPREHSKS ASLLFGMRNS AASDEDSSWA TLSQGSPSYG SPEDTDSFWN
HFE65 PPGLPEPLES VEAPPRPQAL TDGPREHSKS ASLLFGMRNS AASDEDSSWA TLSQGSPSYG SPEDTDSFWN
      281                                                                350
MFE65 PNAFETDSDL PAGWMRVQDT SGTYYWHIPT GTTQWEPPGR ASPSQGSSPQ EESQLTWTGF AHQEGFEEGE
RFE65 PNAFETDSDL PAGWMRVQDT SGTYYWHIPT GTTQWEPPGR ASPSQGNSPQ EESQLTWTGF AHQEGFEEGE
HFE65 PNAFETDSDL PAGWMRVQDT SGTYYWHIPT GTTQWEPPGR ASPSQGSSPQ EESQLTWTGF AHGEGFEDGE
      351                                                                420
MFE65 FWKDEPSEEA PMELGLKDPE EATLSFPAQS LSPEPVPQEE EKLSQRNANP GIKCFAVRSL GWVEMTEEEL
RFE65 FWKDEPSEEA PMELGLKDPE EGTLPFSAQS LSPEPVPQEE ENLPQRNANP GIKCFAVRSL GWVEMTEEEL
HFE65 FWKDEPSDEA PMELGLKEPE EGTLTFPAQS LSPEPLPQEE EKLPPRNTNP GIKCFAVRSL GWVEMTEEEL
      421                                                                490
MFE65 APGRSSVAVN NCIRQLSYHK NNLHDPMAGG WGEGKDLLLQ LEDETLKLVE PQNQTLLHAQ PIVSIRVWGV
RFE65 APGRSSVAVN NCIRQLSYHK NNLHDPMSGG WGEGKDLLLQ LEDETLKLVE PQNQTLLHAQ PIVSIRVWGV
HFE65 APGRSSVAVN NCIRQLSYHK NNLHDPMSGG WGEGKDLLLQ LEDETLKLVE PQSQALLHAQ PIISIRVWGV
      491                                                                560
MFE65 GRDSGRERDF AYVARDKLTQ MLKCHVFRCE APAKNIATSL HEICSKIMSE RRNARCLVNG LSLDHSKLVD
RFE65 GRDSGRERDF AYVARDKLTQ MLKCHVFRCE APAKNIATSL HEICSKIMSE RRNARCLVNG LSLDHSKLVD
HFE65 GRDSGRERDF AYVARDKLTQ MLKCHVFRCE APAKNIATSL HEICSKIMAE RRNARCLVNG LSLDHSKLVD
      561                                                                630
MFE65 VPFQVEFPAP KNELVQKFQV YYLGNVPVAK PVGVDVINGA LESVLSSSSR EQWTPSHVSV APATLTILHQ
RFE65 VPFQVEFPAP KNELVQKFQV YYLGNVPVAK PVGVDVINGA LESVLSSSSR EQWTPSHVSV APATLTILHQ
HFE65 VPFQVEFPAP KNELVQKFQV YYLGNVPVAK PVGVDVINGA LESVLSSSSR EQWTPSHVSV APATLTILHQ
      631                                                                700
MFE65 QTEAVLGECR VRFLSFLAVG RDVHTFAFIM AAGPASFCCH MFWCEPNAAS LSEAVQAACM LRYQKCLDAR
RFE65 QTEAVLGECR VRFLSFLAVG RDVHTFAFIM AAGPASFCCH MFWCEPNAAS LSEAVQAACM LRYQKCLDAR
HFE65 QTEAVLGECR VRFLSFLAVG RDVHTFAFIM AAGPASFCCH MFWCEPNAAS LSEAVQAACM LRYQKCLDAR
      701                                                                770
MFE65 SQTSTSCLPA PPAESVARRV GWTVRRGVQS LWGSLKPKRL GSQTP*RTPI LPLP.ACLGP QGTQGFGAGR
RFE65 SQTSTSCLPA PPAESVARRV GWTVRRGVQS LWGSLKPKRL GSQTP*RAPI LPLP.ACFGP QGTQGFGAGR
HFE65 SQASTSCLPA PPAESVARRV GWTVRRGVQS LWGSLKPKRL GAHTP*RSPH LPFHLIVLGP RELKGVGQGG
      771                                                                840
MFE65 GCGCSSYTPR PLGCPSSVAG VPYLGAGREK LNSFTEVITL D**HEGPEAK PALGSPSPVF EVEQEELVQA
RFE65 GCGCSSYTPC PPGCPSSVAG VPYLGAGREK LNSFTEVITL D**HRGREAK PALGSPSPVF EVEQEELVQA
HFE65 V*RLFLGLRP PKYAPPQ*VR FPA*ELGRER SNPFKEVITL EW*QEEQEAR PALVLHPHVF QVEQEELVQA
      841                                                        889
MFE65 RPHPQRPSRG RR..GLVS.W IPSPLFCG.H LRCTDIT~~~ ~~~~~~~~~
RFE65 RPHPQRPNKG RR..GLVSAW IPCPLFCG.H LHCTDITNKV CLSLKKKKK
HFE65 RPHPPGPSRG RRRKGLVQAW VPSPCSMGTS AVLISLIKSV CT~~~~~~~
```

Figure 2.1. Amino-acid sequence comparison of human, rat and mouse FE65 proteins. The sequence are 98% identical. FE27 Epitope is in purple. FE518 Epitope is in blue. FE352 epitope is in green. The potential translation start codons are in bright green. The translation stop codon are in red. The WW domain is in a rectangle box and are highlighted in bold red. ▲▼ indicates where the exon 2 coding region ends.

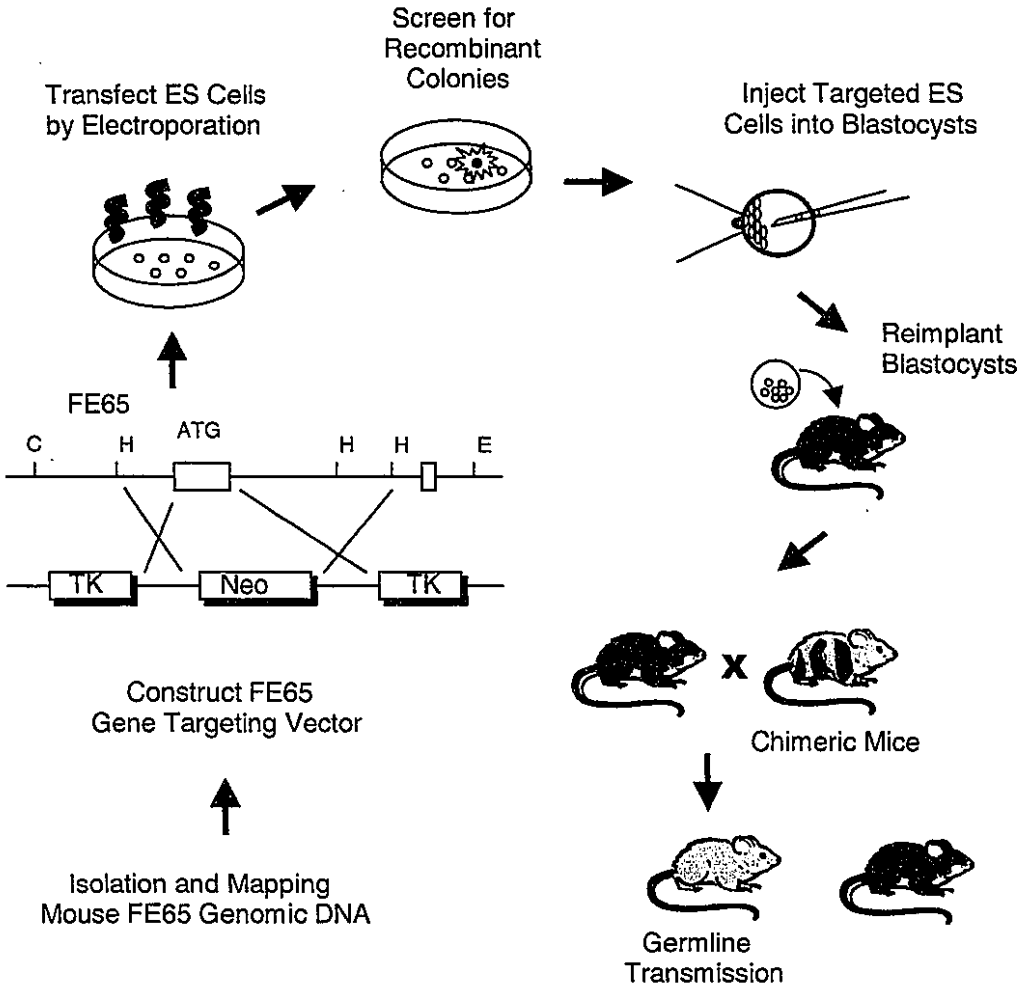

Figure 2.2. Procedure for generating transgenic mice via gene targeting.

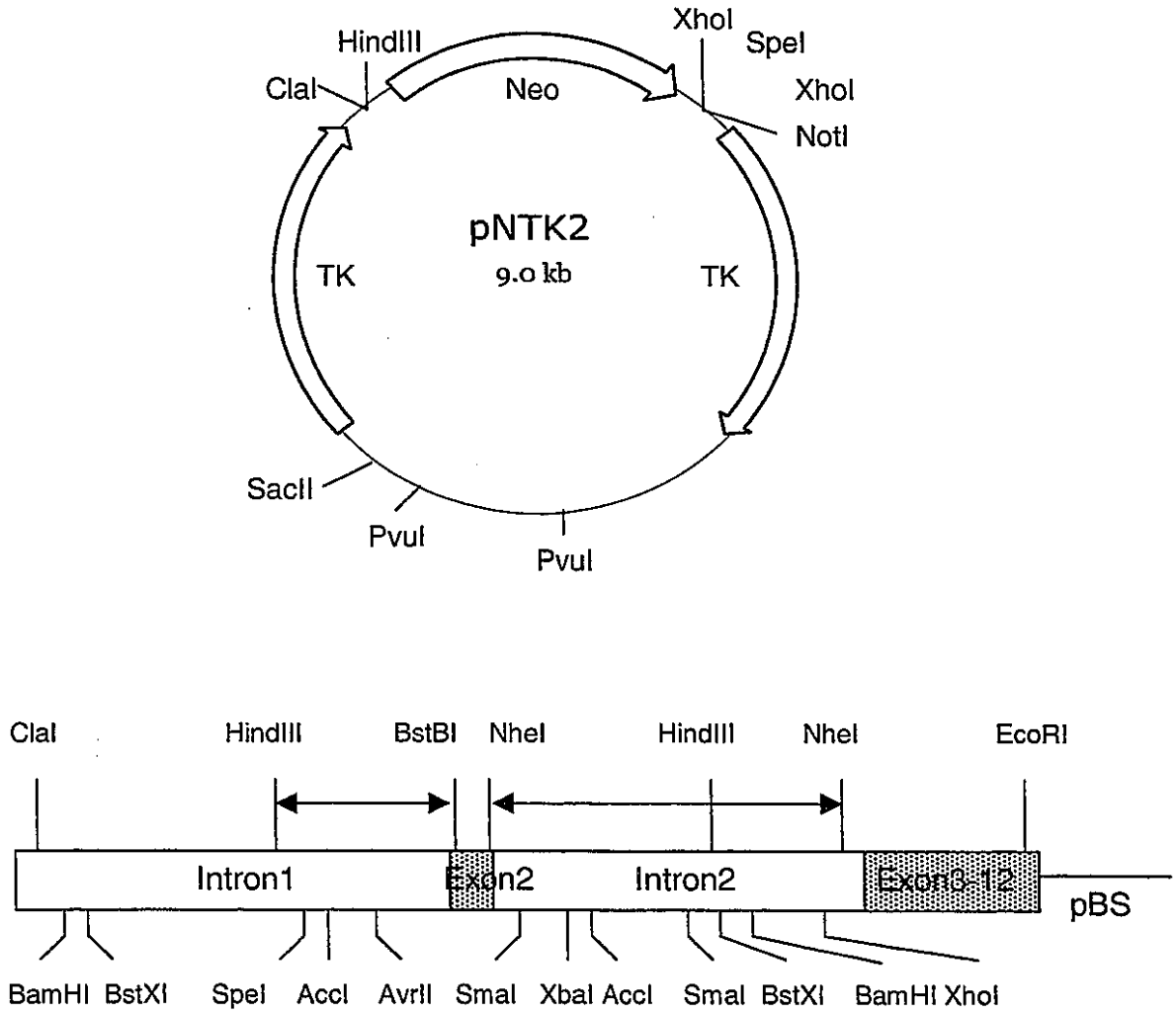

Figure 2.3. Schematic diagram of the pNTK2 targeting vector and the FE65 genomic clone used to generate the targeting construct. FE65 genomic sequence containing part of intron 1 (6 kb) through exon 12 (15 kb total), was subcloned into a NotI site of a pBlueScript vector (pBS; Stratagene, La Jolla, CA), and used to construct a targeting vector. A 2.8 kb HindIII/BstBI fragment including part of intron 1 and the 5' exon 2, and a 5.5 kb NheI fragment containing the 3' exon 2 and part of intron 2 were inserted into the ClaI, and the SpeI sites, respectively, of a pNTK2 gene targeting vector.

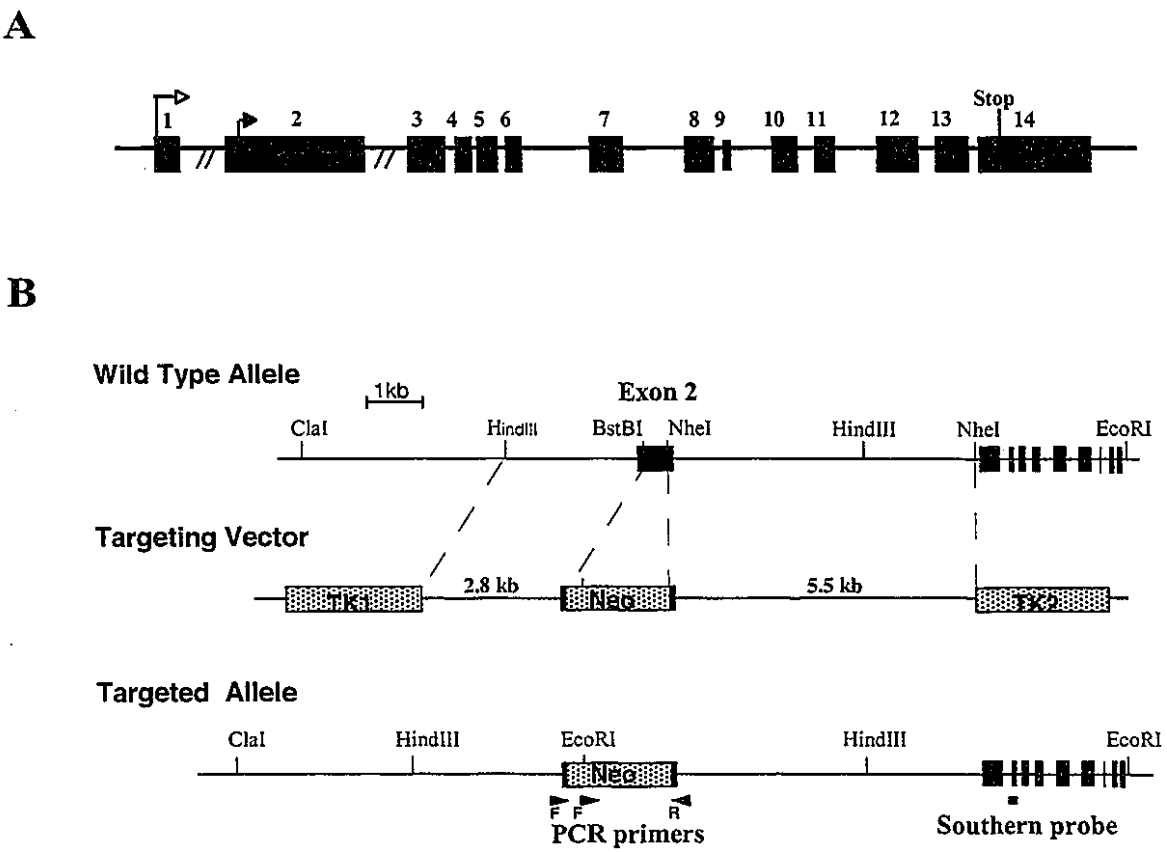

Figure 2.4. *FE65* gene structure and gene targeting strategy. **A.** Structure of the FE65 gene. Exons are indicated by numbered filled boxes. Lines between exons represent introns. Open and filled arrows represent the transcriptional initiation site and translational start site, respectively. The translational stop site is shown by a vertical bar above exon 14 (From Hu et al., 1998). **B.** Schematic diagram of the strategy used to target the *FE65* locus. The structure of the endogenous murine *FE65* gene is shown on the top, and that of the targeting construct is shown on the center panel. Thin horizontal lines represent mouse genomic DNA; filled numbered black boxes represent *FE65* exons. The phosphoglycerate kinase (PGK) promoter-driven neomycin gene (Neo) and the herpes simplex thymidine kinase gene (TK) cassettes are shown as shaded boxes. The translational initiation site of the FE65 protein is indicated. Homologous recombination generates a fusion of the neomycin resistance gene replacing the majority of the exon 2 of the *FE65* genomic sequence including the translational start site. The targeted allele is illustrated at the bottom. Location of the Southern probe fragment and PCR primers for genotyping are indicated.

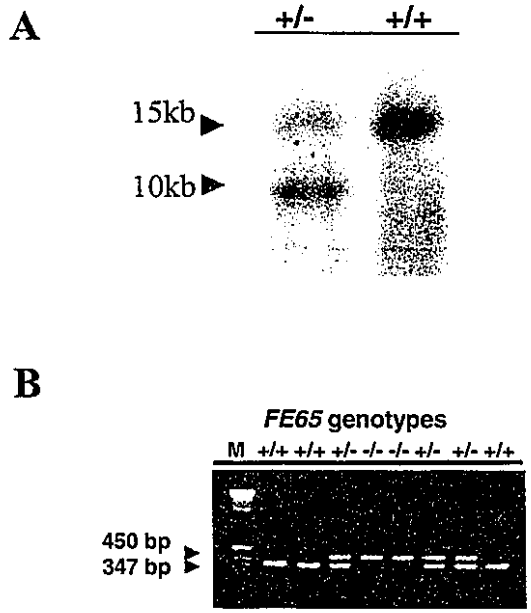

Figure 2.5. Southern and PCR analysis of the targeted gene. **A.** Southern blot analysis of the targeted gene in ES cells. Genomic DNA isolated from ES cells was digested with EcoRI and ClaI restriction enzymes and hybridized with the external probe shown in (Fig 2.4 B). The wild type *FE65* allele generated a 15 kb EcoRI and ClaI fragment, whereas an EcoRI site in the disrupted allele yielded a 10 kb EcoRI fragment. B. Genotypic analysis of the *FE65* locus of targeted mice by PCR. Mouse tail DNA derived from the progeny of heterozygous mutant mice was analyzed by PCR performed with two primer sets in a single reaction tube using the position and orientation of the oligonucleotide primers shown in (Fig 2.4 B). The expected sizes of the amplified fragments were 347 bp for the wild-type allele (+) and 450 bp for the targeted allele (-). M: Molecular weight markers.

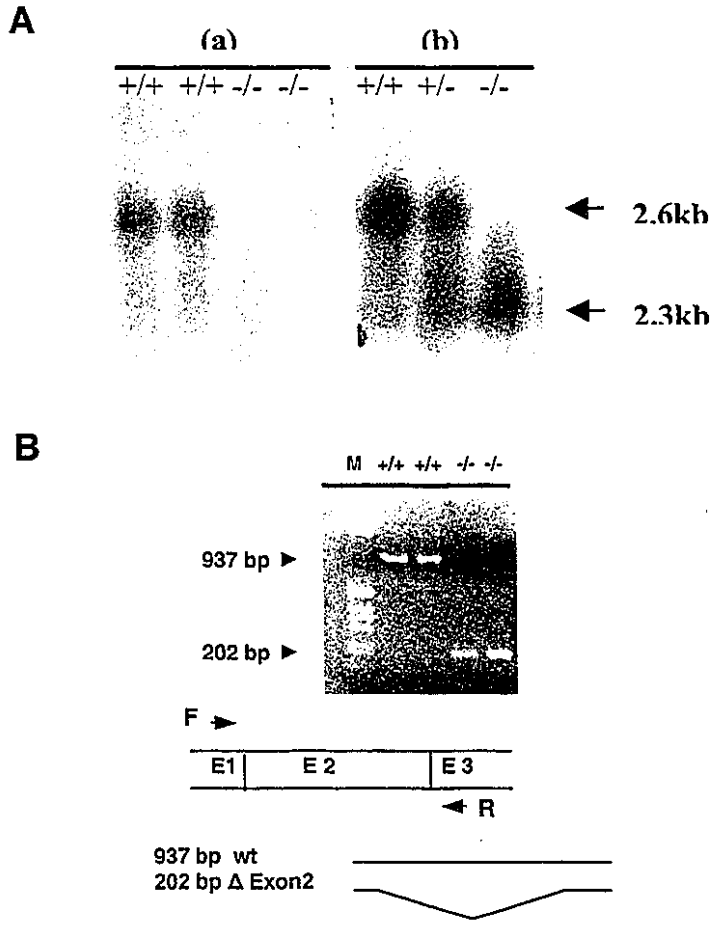

Figure 2.6. Northern and RT-PCR analysis of *FE65* transcripts. **A.** Total RNA from *FE65*$^{+/+}$, *FE65*$^{+/-}$ and *FE65*$^{-/-}$ mouse brains were electrophoretically separated on a 1.2% agarose gel, transferred to a nylon membrane, and hybridized with cDNA probe 1 (680 bp, corresponding to exon 2), shown in (a); hybridization with probe 2 (626 bp, corresponding to exon 11-14), is shown in (b). Both probes hybridized with 2.6 kb mRNA bands, the expected results for wild type *FE65* mRNA. In contrast, the 2.6 kb *FE65* mRNA was not detected in *FE65* knockout mice. **B.** RT-PCR analysis of *FE65* transcripts. Total mRNAs from *FE65*$^{+/+}$, *FE65*$^{+/-}$ and *FE65*$^{-/-}$ mouse brains were reverse transcribed into single stranded cDNAs with random primers, and amplified by PCR. The primer sets amplifying exon 2 and its surrounding regions consisted of a forward primer (F) located on exon 1 and a reverse primer (R) located on exon 3 as indicated. Wild type RNA is expected to yield a 937 bp product and RNA from *FE65* knockout mice (lacking exon 2) is expected to yield a 202 bp product, in agreement with the observed results.

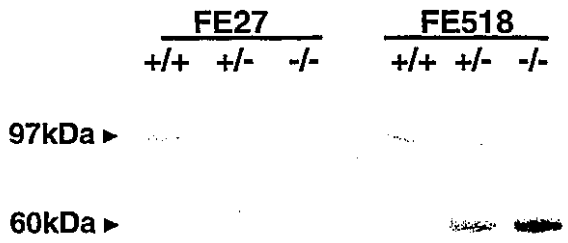

Figure 2.7. Western Analysis of FE65 proteins from crude lysates of mouse brain. Whole brain tissue lysates were separated on 7.5% SDS-PAGE, and immunoblotted with purified anti-FE65 antibodies. The 97 kDa bands representing the full-length FE65 protein were recognized by both FE27 and FE518. Intensities of the bands in p97FE65$^{+/-}$ mice were decreased by 50% when compared with those from wild type mice. The 60 kDa bands recognized only by FE518 were novel N-terminally-truncated isoforms (also see Chapter. 3). FE27: a polyclonal antibody against an N-terminal epitope of FE65; FE518: a polyclonal antibody against an epitope between the PID1 and PID2 domains of FE65.

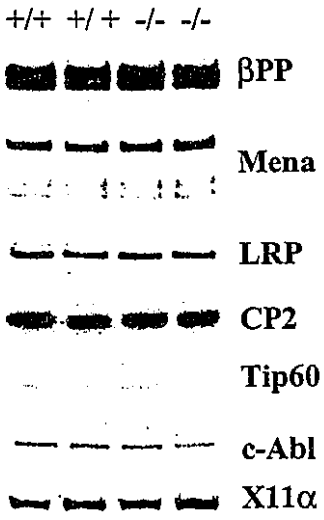

Figure 2.8. Expressions of the FE65 binding proteins and X11α in FE65 mutant mice. The levels of various known FE65 binding proteins and X11α in brains of FE65 mutant mice were analyzed by western blotting. βPP was detected using antibody B994 (anti-βPP C-terminus). Similar results were seen using a different anti-βPP C-terminus antibody and 22C11 (anti-βPP N-terminus) (data not shown). There are no significant differences observed between genotypes.

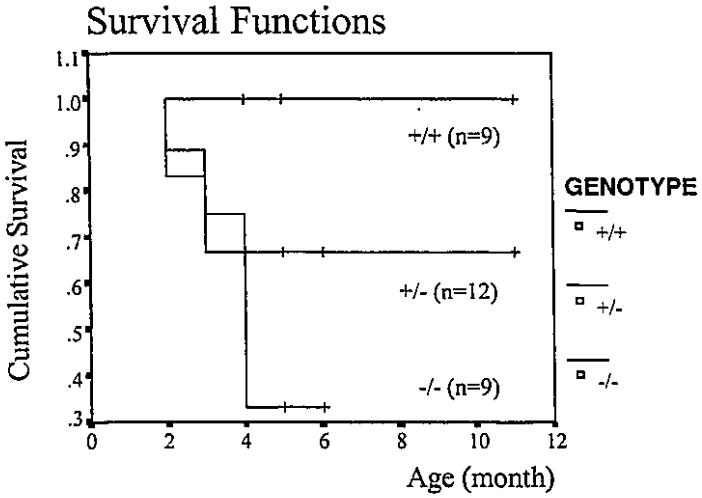

Figure 2.9. Survival analysis of Tg2576 X *FE65* F1 hybrid mice. Male Tg2576 mice heterozygous for *FE65* were mated with female *FE65* heterozygous mice to produce Tg2576 offspring with different *FE65* genotypes. Kaplan-Meier survival curves for these mice are shown. The curves represent 9 $FE65^{+/+}$, 12 $FE^{+/-}$ and 9 $FE65^{-/-}$ mice with the Tg2576 transgene arrays. No Tg2576 mice that were wild type for *FE65* died up to 11 months. Lack of expression of *FE65* decreased survival of outbred mice overexpressing *APP*. The differences between the groups were statistically significant ($P<0.05$).

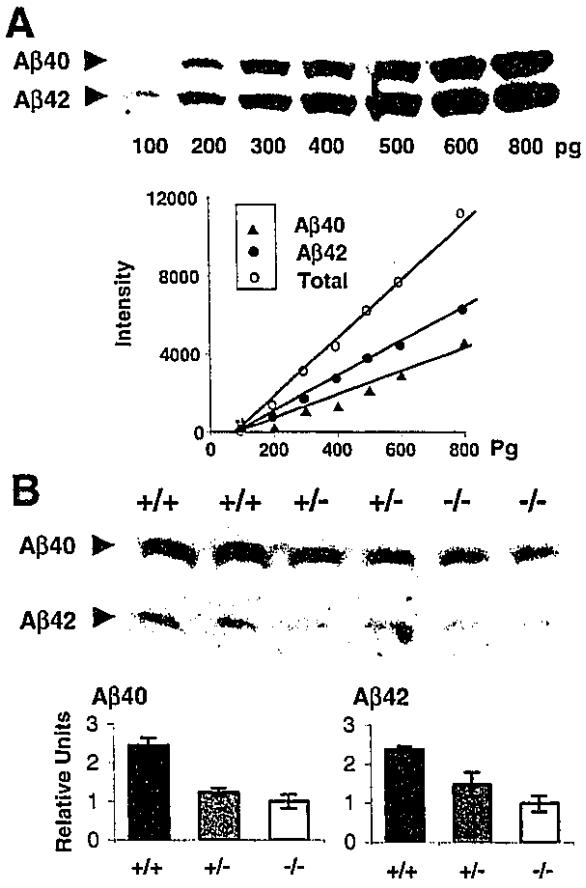

Figure 2.10. Quantitation of Aβ peptides in media from primary neuronal cultures of Tg2576 X FE65 F1 hybrid mice. **A.** Standard curve for quantitation of Aβ40 and Aβ42 peptides using bicine-PAGE and Western analysis. Upper panel: Serial dilutions of standard Aβ peptides were separated on a 16.5% bicine-PAGE gel, transferred to a membrane and immunoblotted with the antibody 6E10. Lower panel: Peptide bands (upper panel) were scanned and quantitated. Intensities of bands were plotted as a function of increasing amounts of loaded peptides. **B.** Decreased levels of Aβ40 and Aβ42 secretion by cultures of primary neurons derived from p97FE65$^{+/-}$ /Tg2576 and p97FE65$^{-/-}$/Tg2576 mice. Upper panel: Primary cortical cultures were generated from neonatal mice (2-48 hr post-natal) from the crossing of p97FE65$^{+/-}$ females and p97FE65$^{+/-}$/Tg2576 males. Eight days after plating, the media were collected and subjected to the bicine-PAGE followed by western analysis. Lower panel: Quantitation of Aβ40 and Aβ42. Data are expressed relative to the results from p97FE65$^{-/-}$/Tg2576 mice and are expressed as the means ±SD (n=4).

CHAPTER 3

IDENTIFICATION AND CHARACTERIZATION OF A NOVEL ISOFORM OF FE65 PROTEIN

3.1. Introduction

FE65 was reported to be protein species of 710 amino acids (molecular mass = 97 kDa) with three protein interacting domains, a WW domian and two PIDs. Alternative splicing of FE65 mRNA was found in the exon 9 region (within PID2), giving rise to two protein isoforms varying only in presence or absence of 2 amino acids (glutamic acid and arginine) (Duilio et al., 1991). The exon 9-inclusive form was exclusively expressed in neurons, while the exon 9-exclusive form was widely expressed in all non-neuronal cells (Hu et al., 1999). In the process of generating and characterizing a mouse strain carrying a disrupted *FE65* locus, we unexpectedly identified a previously undescribed native isoform of FE65 protein in mouse brains, apparently produced via internal translation initiation. This newly identified FE65 isoform (p60) differs from the full length FE65 (p97) in several aspects including expression pattern and cellular localization. Therefore, p60 is likely to be of physiological significance.

3.2. Materials and Methods

3.2.1. Western Analysis and GST Pull Down Assays

Affinity-purified rabbit polyclonal antibodies against FE65 were used (Hu et al., 2002). Antibody FE27 recognizes an N-terminal epitope (amino acids 27-36: PLHAAHNQLL), immediately downstream of the first AUG codon in the open reading frame (ORF) of *FE65*. Antibody FE518 recognizes a C-terminal epitope (amino acids 518-527: LDHSKLVDVP) between the PID1 and PID2; antibody FE352, a gift from Affinity BioReagents (Golden, CO), recognizes a region upstream of the PID1 (amino acids 352-369: PQEEEKLSQRNANPGIK) (Fig. 3.1). All the epitope sequences are conserved between human and mouse; none of them have homology with other family members, FE65 L1 and FE65 L2. Mouse whole brains were dissected on ice and homogenized at 100 mg/ml in a cold lysis buffer (50 mM Tris HCl, pH 7.4, 150 mM NaCl, 0.5% Triton-X100, 10% glycerol, 50 mM NaF, 1 mM sodium vanadate) supplemented with a protease inhibitor cocktail, Complete EDTA-free™ (Roche, Palo Alto, CA). For pull down assays, brain lysates were subjected to affinity purification with a fusion protein between Glutathione S-transferase (GST) and the C-terminal 48 amino acids of the human βPP (GST-βPP-C48), followed by Western analysis (Hu et al., 2002).

3.2.2. Cytoplasmic and Nuclear Fractionation

The preparation of cytoplasmic and nuclear extracts was performed using a Nuclear Extract Kit (ActiveMotif, Carlsbad, CA) according to manufacturer's instruction. Briefly, fresh cerebral cortices from half hemisphere of a 2 months old wild type and FE65 mutant mouse were diced and homogenized in 1.5 ml hypotonic buffer using a Dounce homogenizer. Supernatants were harvested as cytoplasmic fractions. Pellets were resuspended in 50 ul of Complete Lysis Buffer and centrifuged at 14,000 x g for 10 min at 4C; supernatants were saved as the nuclear fractions.

3.3. Results

3.3.1. Identification of a Novel Isoform of FE65 Proteins (p60)

Western blot analysis with antibodies specific to the N-terminus (FE27) or to the C-terminus (FE518) of FE65 revealed the presence of an additional uncharacterized FE65 species with an apparent molecular mass of 60 kDa in the brain lysates of both wild type and *FE65* mutant mice. Direct Western analysis demonstrated that the 60 kDa bands could be recognized by FE518 but not by FE27 (Fig. 3.1), suggesting that the bands might be a N-terminally truncated FE65 isoform (Fig. 3.1). The results from GST-βPP-C48 pull-down assays were consistent with the observations of direct Western analysis. As shown in Fig, 3.1, both 97 kDa and 60 kDa FE65 proteins were enriched by GST-βPP-C48 pull down; the 97 kDa isoform was recognized by both FE27 and FE518 while the 60 kDa isoform was only recognized by FE518. To further characterize the 60 kDa bands, an additional FE65 antibody FE352 whose epitope is

localized at the beginning of the PID1 was used. Although FE352 is not strong enough for direct Western analysis (data not shown), it could easily recognize both 97 kDa and 60 kDa FE65 proteins in pull-down materials (Fig. 3.1). Because none of these epitopes have homologous residues with the other FE65 family members, we conclude that the 60 kDa fragment is derived from the same ORF of *FE65* gene. We therefore refer to the 97 kDa full-length FE65 protein (710 amino acids), initiated from the first ATG codon, as p97, and the 60 kDa protein as p60.

Since exon 2 (containing the first translation initiation codon) has been deleted in *FE65* mutant mice, p60 may be a product of alternative translation from an internal in-frame initiation site. Examination of the FE65 coding sequences revealed the presence of two such potential ATGs, methionine 260 (M260) and methionine 327 (M327) in the region from the beginning of exon 3 to amino acid 352 (the beginning of the epitope for FE352). p60 is likely translated from M260 since it corresponds to the first available AUG in the mRNA of *FE65* mutant mice (Kozak, 2002). Therefore, p60 would lack more than one-third of the N-terminal residues of p97, including part of WW domain, but would retain two PID domains. The evidence that p60 is also expressed in the wild-type-mouse brains suggests that M260 is an active internal translation-initiation site, and that p60 is, by definition, a physiologically relevant product in mouse brain.

3.3.2. Increased Binding Affinity of p60 for the beta amyloid precursor protein intracelluler domain (AICD)

Using GST-βPP-C48 pull-down assays, we observed significantly increased ratios of p60/p97 in pull-down materials when compared to those of starting brain lysates (Fig 3.1), suggesting that p60 have higher binding affinity to AICD than p97.

3.3.3. Differential Expressions of FE65 Isoforms In Vitro

In order to determine whether p60 is also expressed *in vitro*, COS cells were transfected with a full-length mouse *FE65* cDNA; cell lysates were analyzed in parallel with mouse brain lysates (Fig. 3.1). In transfected COS lysates, protein bands at 97 kDa were observed, which were identical in size to native p97 in brain lysates. In contrast, the p60 bands, were not detected in transfected COS lysates with antibody FE518 (Fig. 3.1). Instead, a ~65 kDa band cross-reacted with this antibody. Further characterization of the 65 kDa band is described in a separate manuscript (Hu et al., in preparation). Failure to produce p60 in the culture system suggests that additional factors may be required for such translation, e.g. tissues-specific factors, as demonstrated by the following experiments.

3.3.4. Cytoplasmic Localization of p60

Previous studies suggested that the N-terminal region of FE65 contains a putative nuclear localization element (Minopoli at al., 2001) and is required for gene transactivation via AICD (Cao and Südhof, 2001). We, therefore, tested whether

endogenous p60 could be targeted to the nucleus by fractioning cytoplasmic and nuclear extracts of cerebral cortex. Western analysis using antibody FE518 revealed that p60 was highly enriched in cytoplasmic extracts (Fig. 3.4) compared to those of non-fractioned cerebral regions (Fig. 3.2); there were no detectable levels of p60 in nuclear extracts. Although p97 was also not detected in nuclear extracts, it might reflect the fact that only a very small portion of the isoform actually translocates into the nucleus *in vivo* to perform nuclear functions (Kesavapany et al., 2002).

3.3.5. Brain-Region Specific Expressions of p60

To examine distribution patterns of the two isoforms in different brain regions, cerebral cortex, hippocampus and cerebellum were dissected from brains of 2-month old mice. Western analysis revealed that p97 was expressed in the lysates of all the examined brain regions of wild type mice, with comparable levels in cortex and cerebellum and relatively low levels in hippocampus when normalized to levels of β-actin (Fig 3.2). Expressions of p60, however, were dramatically different in these brain areas. High levels of p60 were detected in cortex, with ratios of p60/p97 of approximate 1:2. In contrast, levels of p60 in cerebellum were not detectable. In hippocampus, both isoforms were detected at ratios of p60/p97 similar to those of cortex while total amounts of FE65 were only ~10% of those in cortex, which may reflect specific expression of FE65 only in a subset of neurons of this brain region (Kesavapany et al., 2002). These results suggest that the predominant expression of p60 in cortex and hippocampus may be related to their special functions in cognition.

3.3.6. Age-Related Expressions of FE65 Isoforms

Next, we assessed expressions of FE65 isoforms during development and aging. Our results revealed age-associated changes in levels of p97. Whole brain lysates of newborn (postnatal day 1), juvenile (3-week old), young adult (3-month old), middle aged (12-month old) and aged (24-month old) mice were examined for expressions of FE65. Western blotting showed that low levels of p97 were expressed at postnatal day 1, after which levels of p97 were steadily increased and reaching peak levels at 3-month old (Fig. 3.3). These data are consistent with previous observations using a different FE65 antibody (Kesavapany et al., 2002). Expression of p97 was somewhat reduced by middle age and dramatically reduced at the advanced age of 24 months (Fig. 3.3). In contrast, expressions of p60 were not significantly changed over the life course. These observations suggest that alterations of p97 levels may contribute to modulations of cognitive functions over the life span.

3.3.7. Tissue Distributions of FE65 Isoforms

To explore the possibility of p60 expression outside the brain region, various tissues from both wild type and FE65 mutant mice were subjected to western analysis using our sensitive FE65 antibodies. p97 was found in brain and lung using both FE27 and FE518; p60 was not found in the tissues tested except for the brain (Fig. 3.5).

3.4. Discussion

We have speculated that the 60 kD isoform of FE65 result from use of an alternative translational initiation site. The *FE65* message apparently can initiate translation at two different ATG codons. One starts from the first ATG in exon 2 and the other starts from the ATG at codon 260 in exon3 (M260). Alternative translational initiation can occur via two different mechanisms, leaky ribosomal scanning, or internal ribosomal entry (IRES) at multiple AUG sites, as occurs in various viral systems and some eukaryotic mRNAs. If the leaky scanning mechanism would be used for translational initiation of p60, the ribosomal complex should scan ~1200 nucleotides and bypass 14 ATG codons to initiate protein synthesis at M260. Moreover, several of the ATG codons upstream of M260 have preferred consensus sequences (A/G^{-3} and G^{+4}; Kozak, 1996) (Table 1). These are not compatible with the leaky scanning mechanism (Kozak, 2002). Therefore, we favor the IRES mechanism for the formation of the p60 isoform. Alternatively, the 60 kD protein band could represent a novel cross-reactive member of the FE65 family which binds to βPP-C48. This possibility, however, is very unlikely, since all three FE65 specific antibodies recognize the p60 isoform.

Based on the size of protein, the sequences of FE65-specific epitopes, and the ability to bind to the C-terminal of βPP, we propose that p60 is a newly identified native, physiologically significant FE65 isoform expressed in both *FE65* wild type and mutant mice via use of an internal initiation codon within the same ORF. Although the potential regulation and biological significance of the alternative translation remains to

be determined, we have demonstrated that p60 could be found in the cortex and hippocampus, regions associated with major modulations of cognitive functions; in contrast, this isoform was not found in the cerebellum of wild type mice. These expression patterns suggest that translation of p60 is regulated in a tissue-specific manner, consistent with current views that translation from an internal ribosomal entry site is often regulated by physiological activity (Dyer et al., 2003), cell cycle (Cornelis et al., 2000; Sachs, 2000), or stress (Holcik et al., 2000). Although translations of p60 in wild type and mutant mice may start from the same codon, the mechanism for regulating the translation in mutant mice might be slightly different because p60 may use the first available AUG (M260) rather than an internal ribosomal entry site. This may be relevant to the observed increased levels of expression of the isoform in mutant as compared to wild type mice. We have previously reported that a polymorphism in human *FE65* intron 13 that influences alternative splicing of exon 14 is associated with resistance to very late onset Alzheimer disease (Hu et al., 2002). We should point out that alternative splicing of exon 14 and the generation of p60 may be two independent events. The former results from the presence or absence of an intron 13 polymorphism. It produces two isoforms (FE65 and FE65a2) of similar sizes (~97 KDa) with 53 C-terminal amino-acids that are characteristic of each isoform (Hu et al., 2002). The latter (p60) may be due to alternative translation from exon 3. It generates a smaller protein with a truncated N-terminus.

As discussed before, if p60 was translated from M260, it would lack part of the WW domain, but retain two PID domains. Its altered structure suggests that p60 may be functionally divergent from p97. For example, it may or may not efficiently bind to Mena, as this action requires the WW domain (Ermekova et al., 1997). Previous evidence has shown that an experimentally induced N-terminally truncated FE65 (lacking amino acids 1-286) could not trigger gene transactivation of AICD in the nucleus (Cao and Südhof, 2001), probably due to the absence of a putative nuclear localization element at amino acids 250-290 around the WW domain (Minopoli at al., 2001). In addition, p60 showed a greater binding affinity to AICD than its longer counterpart (Fig. 3.1). It has been proposed that βPP might serve as an anchor molecule in the cytosol to prevent FE65 from getting into the nucleus (Minopoli et al., 2001; Cao and Südhof, 2001). Thus, p60 may have an additional obstacle for translocation into the nucleus. In fact, in the present studies, we showed that p60 was cytoplasmic and could not be detected in the nuclear compartment. Therefore, p60 may have unique unknown cytosolic functions in cytosol, but would lack nuclear functions such as transcription activation and cell cycle regulation (Cao and Südhof, 2001; Bruni et al., 2002).

Overexpression studies and the generation of p60-specific knockout mice may shed light on the function of p60. Its N-terminal structure needs to be further analyzed by microsequencing. The translational control of p60 via IRES and its regulation is another interesting area that needs further investigation. It is conceivable that aberrant

regulation or function of p60 is associated with disease states. In any case, the discovery of this novel isoform would certainly enhance our understanding of the diversity and complexity of FE65 function.

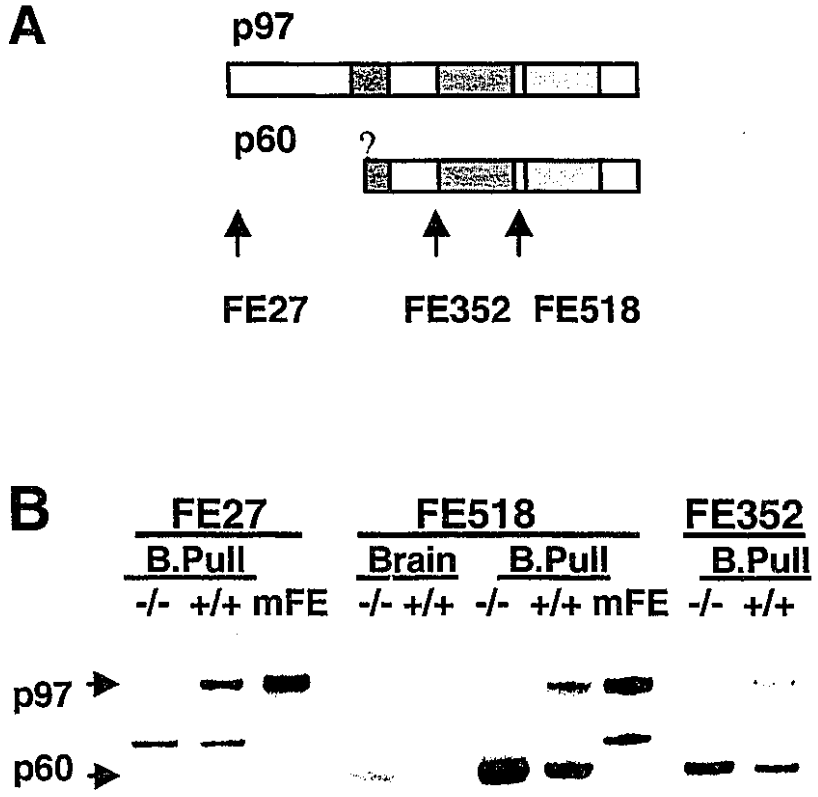

Figure 3.1. Western and GST-pulldown analyses of expressions of FE65 isoforms. **A**, Schematic diagram of the epitope positions of FE65 antibodies and the domain structures of the full-length (p97) and N-terminally-truncated (p60) FE65 isoforms. Arrows indicate the positions of epitopes that are recognized by FE27, FE352 and FE518. ?: the precise site of the N-terminal truncation is unknown. **B**, Brain tissue lysates from p97*FE65*$^{+/+}$ and p97*FE65*$^{-/-}$ mice were analyzed by direct Western blotting or by GST-βPP-C48 pull-down followed by Western blotting with antibodies indicated in (A). B.Pull: GST-βPP-C48 pulled down materials from brain lysates; mFE: COS cell lysates overexpressing a mouse *FE65* cDNA.

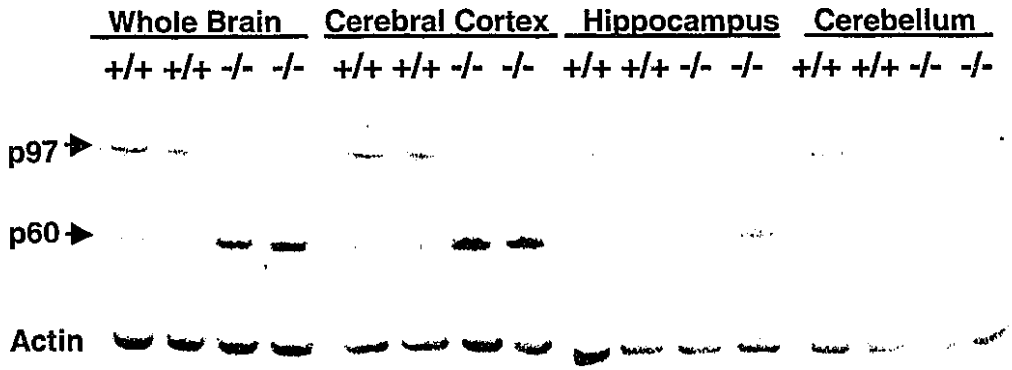

Figure 3.2. Brain region-specific expressions of p60. Cerebral cortex, hippocampus and cerebellum were dissected from 2-month old mouse brains and analyzed by Western blotting with FE518. Whole brain lysates were also analyzed in parallel. The same membranes were then stripped and incubated with an antibody against β-actin as sample-loading controls.

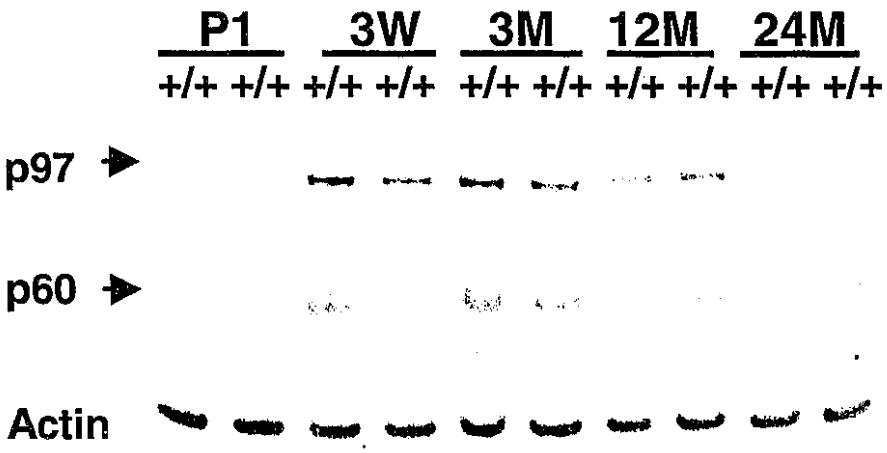

Figure 3.3. Expressions of FE65 isoforms during development and aging. Brain lysates from mice of different ages were analyzed by Western blotting with FE518. The stripped membranes were then incubated with an antibody against β-actin. P1: first post natal day; W: week; M: month.

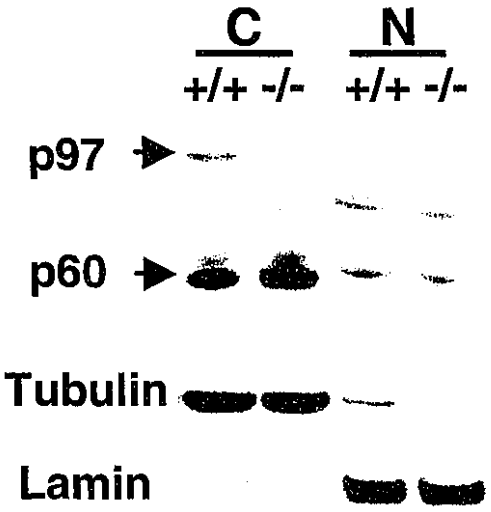

Figure 3.4. Subcellular localizations of endogenous FE65 proteins in mouse brains. Cytoplasmic (C) and nuclear (N) extracts of cerebral cortex of wild type and FE65 mutant mice were separated using a nuclear extract kit, and analyzed by immunoblotting with FE518, and with anti-Lamin A+C antibody (Chemicon, Temecula, CA) and anti-tubulin antibody (Sigma, St Louis, MO) as positive controls for nuclear and cytoplasmic fractions, respectively. p60 were only detected in the cytoplasmic extracts. The bands shown in the nucleur extracts were nonspecific bands that migrates slower than the p60.

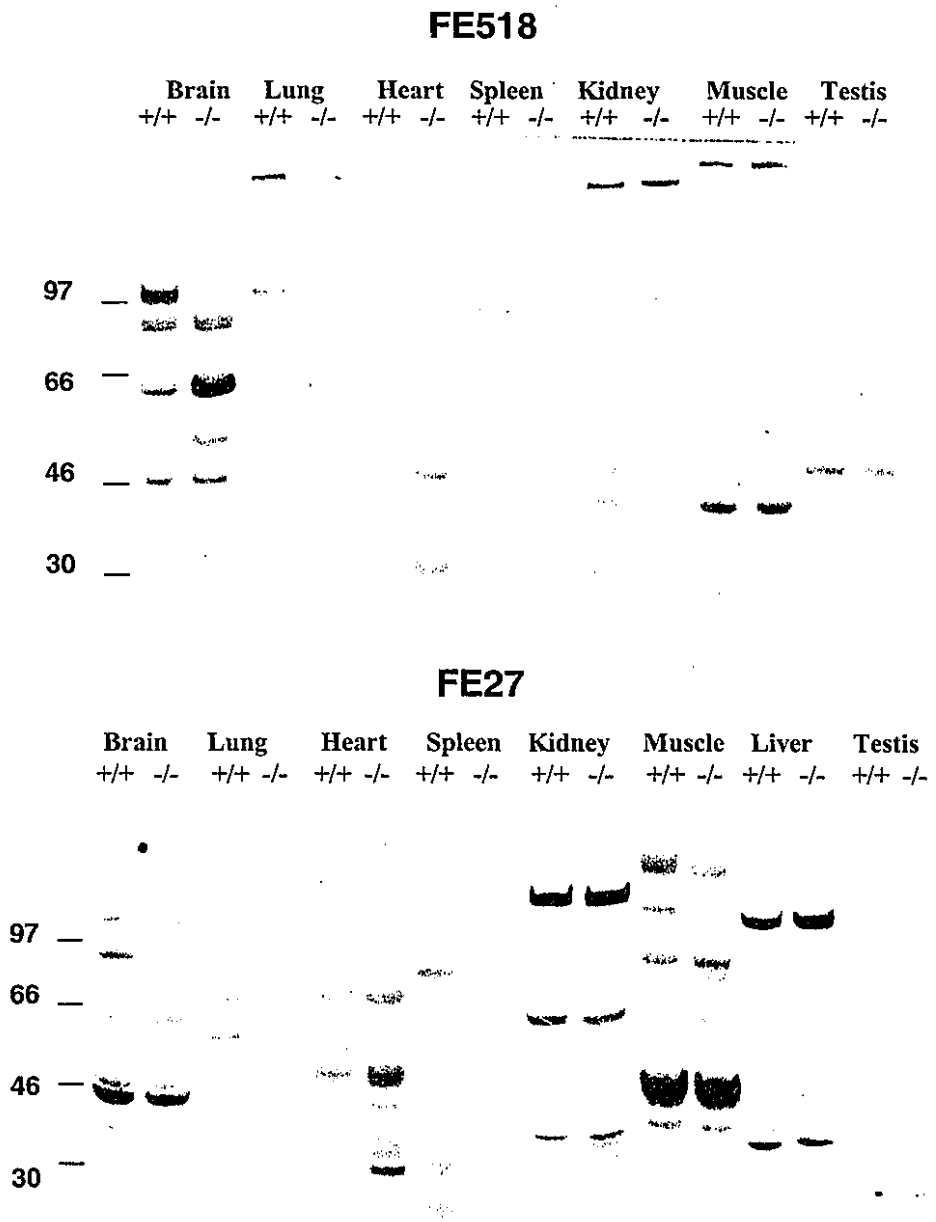

Figure 3.5. Tissue Distributions of FE65 isoforms. Various tissues from both wild type and FE65 mutant mice were subjected to western analysis using FE65 antibodies: FE518 and FE27.

Table 1. Survey of ATG Codons and Their Flanking Nucleotides Within the First 1200 Nucleotides of the p97FE65 cDNA

ATG Number	ATG Context (CC[A/G]CCatgG)	In Frame ATG Position
1	AGGCCatgT	M1
2	GTGCTatgG	M54
3	TGCCAatgC	
4	CCGAAatgT	
5	GCTTAatgC	M114
6	CCACAatgC	
7	GCTTCatgG	
8	ACCAGatgA	
9	GGAGGatgA	
10	GGATGatgA	
11	GGAGAatgT	
12	TTGGCatgC	M212
13	CAGTGatgA	
14	TCCCTatgG	
15	GCTGGatgA	
16	GATGGatgA	M260
17	GAAGGatgA	
18	CCCCAatgG	M327

Matches with the consensus sequence are shown in red.

CHAPTER 4

BEHAVIORAL ANALYSIS OF FE65 MUTANT MICE

4.1. Introduction

Since FE65 is predominantly expressed in the hippocampus and cerebellum, brain structures that influence important behaviors such as learning and memory, locomotion, and coordination, we performed tests for these phenotypes. Two different tests for learning and memory were used, passive avoidance and Morris Water Maze (Fig 4.1). Loss of the full-length FE65 but not a N-terminally truncated isoform in the mutant mice was associated with impaired performance in tests of learning and memory. Deficiencies in a reversal-learning paradigm were particularly striking. These were reminiscent of "unforgetting" phenotypes that were previously observed in mice bearing conditional null mutation of presenilin 1 (PS1), a member of the γ-secretase complex (Feng et al, 2001). Our studies thus suggest a novel role for FE65 protein in learning and memory.

4.2. Materials and Methods

4.2.1. Animals

All of the mice used for the behavioral studies were F_2 progeny derived from matings of F1 heterozygotes (129/Sv × C57BL/6J). The animal experiments were approved by the U.S. National Institutes of Health and by the University of Washington Animal Care and Use Committee. Mice were group-housed by gender in a temperature- and humidity-controlled specific pathogen-free facility. All mice were tested within the light phase of a 12 h light/dark cycle.

4.2.2. Open Field Test

Locomotor activity was measured using an open field apparatus (25.4 × 25.4 × 40.6 cm; Coulbourn Instruments, Allentown, PA) and analyzed by Tru-Scan 99 software (Coulbourn Instruments, Allentown, PA). Animals were placed in the center of the apparatus for 10 min in standard room-lighting conditions. Three dependent variables recorded by the software were reported in Results: (1) the total distance traveled in cm, (2) the relative amount of time spent in the center, and (3) the number of rearings. Between sessions, the cage was wiped clean with 70% ethanol.

4.2.3. Passive Avoidance Learning

Experiments were conducted as previously described (Wong et al., 1999). A passive avoidance apparatus (Fig. 4.1; Coulbourn Instruments, Allentown, PA) was used, which consisted of one darkened compartment and one illuminated compartment separated by a guillotine door. The floor consisted of a metal grid wired to deliver shocks of controlled intensities and durations. During testing, each mouse was placed

into the illuminated compartment of the apparatus and allowed to explore for 1 min. The door to the dark compartment was then opened. Step through latencies, defined as the time required for the mouse to cross completely to the darkened compartment, were recorded for the mouse. Ten minutes after the mouse entered the dark compartment, the door was closed, and the mouse received a 0.7 mA shock of 2 sec duration. Mice were allowed to recover from the shock for 30 sec and then returned to their cages. This test was performed over a period of 6 consecutive days at the same time during each day. The latency to enter the dark compartment was monitored for each trial. Mice were removed if they failed to enter the dark compartment after 10 min and were assigned a latency of 600 sec. A learning score, indicating the day (1 to 7) when a mouse first reached 600 sec latency, was assigned to each mouse and used to assess acquisition of the task (score as 1 if 600 sec latency was reached on day 1 and so on; 7 was assigned if 600 sec latency was never reached). The apparatus was wiped down with 1% acetic acid between trials.

The sensitivities of the groups of mice to increasing foot shock intensities were assessed as published (Wong et al., 1999). Mice were scored for flinching, jumping and vocalization responses to shocks of 1 sec duration ranging from 0.06 to 0.5 mA.

4.2.4. Morris Water Maze (MWM)

Hidden Platform Test. The water maze was a circular pool 1.2 m in diameter filled with water, maintained at 22°C, and rendered opaque by addition of non-toxic white

paint. A 10 cm diameter escape platform was submerged 1 cm beneath the water surface at a fixed location throughout the course of the hidden platform tests. On each trial, the mouse was placed facing along the edge of the wall and randomly released at three start points. Mice were allowed to swim freely until they climbed onto the platform or until 60 sec had elapsed, at which point they were placed on the platform for 15 sec. Mice were given one block of four trials a day, with a 1 min inter-trial interval each day, for 9 consecutive days. During each trial, the time to find the hidden platform was recorded and averaged daily. A video camera was mounted above the pool and mouse movements were tracked with a computerized video-tracking system (Fig 4.1).

Reversal Test. Reversal of spatial learning was tested on day 11-13. During this phase, the platform was placed in the opposite quadrant from where it had previously been. As in the prior phase, 4 trials per daily session were conducted.

Probe Test. A single probe test was carried out on the days after the completion of the hidden platform test (day10) and the reversal test (day14). The platform was removed from the maze; mice were placed and released at the location opposite the site where the platform had been located. Each mouse was allowed to swim for 60 sec. The number of entries into the target area (where the platform had been positioned) and the time spent in each quadrant were recorded.

Visible Platform Test. The experimental set-up for the visible portion of the MWM was as above, except that the platform was raised just above the level of the water and a flag was attached to the platform. The platform location was varied randomly from trial to trial. Each mouse was given four trials for three days, and the time to find a platform was recorded and averaged.

4.2.5. Statistics:

Behavior tests were analyzed by one or two factor analyses of variance (ANOVA). Newman-Keuls post hoc analyses were performed when necessary. Passive avoidance acquisition curves were analyzed by the two-sample Wilcoxon rank-sum (Mann-Whitney) test. The water maze performance curves were analyzed by repeated measures ANOVA. All the analyses were carried out using the STATA software (Stata Corporation, College Station, TX). All values are given as ± SEM.

4.3. Results

To test the hypothesis that altered expression of FE65 could contribute to cognitive impairments, a series of behavioral tests for assessment of learning and memory was performed. Since no statistically significant differences in performance on any of these tests were observed between genders, all data were collapsed into single groups of p97FE65$^{+/+}$, p97FE65$^{+/-}$ and p97FE65$^{-/-}$ mice. The apparently normal development, histology and life spans of *FE65* mutant mice suggested that the interpretation of

behavioral tests of complex cognitive functions in these mice would not be clouded by developmental and adult pathologies.

4.3.1. Normal Performance in the Open Field Test

Because most well-established behavioral paradigms rely upon locomotion, it is important to rule out an underlying defect in locomotor activities. As a simple test for the spontaneous locomotor activity, mice were monitored using an open-field test (Crusio et al., 1989). The test has been used to reveal gross differences related to activity levels and coordination (Crawley and Paylor, 1997; Picciotto and Wickman 1998). In addition, the open-field test also measures anxiety levels, as assessed by the rearing and the center to perimeter residence time (Treit and Fundytus. 1988; Steiner et al., 1997; Angrini et al., 1998; Ramboz et al., 1998). With this test, levels of general activity were evaluated by measurements of horizontal activity, vertical activity, and total distance traveled during a 10 min test session in an open box in a lighted room. We observed no significant differences, among genotypes, in total distances traveled in the first and second 5 min intervals among genotypes for 14- and 27- month old mice (Fig. 4.2 A. $F_{(2,18)} = 0.75$, $p = 0.4861$; $F_{(2,29)} = 1.69$, $p = 0.2028$). All groups showed habituation to the novel environment, as demonstrated by decreasing activities during the second 5 min interval (14 months: $F_{(1,18)} = 33.54$, $p < 0.0001$; 27 months: $F_{(1,29)} = 19.14$, $p = 0.0001$). $FE65^{+/+}$, $FE65^{+/-}$ and $FE65^{-/-}$ mice exhibited comparable levels of anxiety, as shown by similar residence times in the central ring of the open field (14 months: $F_{(2,18)} = 0.08$, $p = 0.92$; 27 months: $F_{(2,29)} = 1.49$, $p = 0.2421$) (Fig. 4.2

B.). The number of rearing episodes was also very similar for all of the groups (for 14 months: $F_{(2,18)}=1.01$; $p=0.3825$; for 27 months: $F_{(2,29)}=1.01$; $p=0.3769$) (Fig. 4.2 C.). In summary, the results indicate that the genotypes of interest did not differ significantly in levels of general activity and anxiety.

4.3.2. Impaired Passive Avoidance Learning

We then investigated passive avoidance response. This conditioning paradigm elicits robust associative learning that involves the hippocampus (Subley-Weatherly et al., 1996). An aversive stimulus (a mild foot shock) was paired with entry into a dark chamber within a novel environment. We first tested foot shock sensitivities of the mice to evaluate their responses to the stimulus. The three groups of mice exhibited comparable responsiveness to foot shock as assessed by recording the amount of flinching, jumping, or vocalization to increasing stimulus intensities (0.06 mA - 0.5 mA) (Fig. 4.3 C.). We then tested passive avoidance conditioning for mice at 14 months and 27 months of age by delivering a 0.7 mA foot shock of 2 sec duration and recording the crossover latencies. *FE65*$^{-/-}$ and *FE65*$^{+/-}$ mice showed retarded acquisition of the passive avoidance response at 14 months of age (Fig. 4.3 A.). One-way ANOVA analysis of the data from the first day of testing showed that *FE65*$^{+/+}$ and *FE65*$^{-/-}$ mice entered the dark compartment with similar latencies ($F_{2,21}=1.25$, $p=0.3077$). When mice were tested twenty-four hours later, however, the latencies of the three groups were significantly different ($F_{2,21}=3.77$, $p=0.04$); *FE65*$^{+/+}$, *FE65*$^{+/-}$ and *FE65*$^{-/-}$ mice displayed relatively long, intermediate and short delays, respectively,

before entering the dark environment (Fig. 4.3 B.). The groups also differed significantly on day 3 ($F_{2,21}$=4.93, p=0.0176) but not on day 4 or on subsequent days. Acquisition rate of this task over 6 days was further analyzed by the Wilcoxon rank-sum test using the learning score as an index. A learning score (1 to 7) was defined as the number of days it takes for a mouse to learn to avoid the dark compartment completely (when 600 sec latency was reached). *FE65*$^{-/-}$ and *FE65*$^{+/-}$ mice spent significantly longer times to learn this task as compared to *FE65*$^{+/+}$ mice (z=2.767, p=0.0057 and z=2.304, p=0.0212 respectively). *FE65*$^{-/-}$ and *FE65*$^{+/-}$ mice were statistically indistinguishable in this test.

Mice at 27 months of age were also tested for passive avoidance response. Both *FE65*$^{+/+}$ and *FE65*$^{-/-}$ mice at 27 months showed increased crossover latencies over 6 days of the test period (Fig. 4.3 A. and B. $F_{5,110}$=9.17, p<0.0001). However, the Wilcoxon test comparing the two groups revealed no significant difference, although the data for *FE65*$^{-/-}$ suggested a tendency for better performance, (z=-1.124, p=0.2609).

4.3.3. Impaired Performance in the Morris Water Maze

The three genotypes were tested in the MWM, a hippocampus-dependent paradigm (Morris, 1982) employed for the assessment of the ability to acquire, process, and recall spatial information by using escape latency as an indicator of learning. Due to the physical demands of this assay, only 14-month old mice were utilized.

Hidden Platform Acquisition:

FE65$^{-/-}$ mice performed poorly in this test as manifested by significantly longer latencies for locating the platform compared to *FE65*$^{+/+}$ mice (Fig. 4.4 A.). A repeated measure two-way ANOVA analysis comparing the *FE65*$^{+/+}$ and *FE65*$^{-/-}$ mice showed significant effects of genotypes ($F_{1,17}$=5.66, p=0.0294), significant effects of days ($F_{8,136}$=16.69, p<0.0001), and a non-significant interaction ($F_{8,136}$=1.09, p=0.3739), indicating differential performances for the *FE65*$^{+/+}$ and *FE65*$^{-/-}$ mice over the 9 training days. Subsequent pair-wise comparisons revealed that the *FE65*$^{-/-}$ mice had significantly longer escape latencies than the *FE65*$^{+/+}$ mice during the seventh and ninth day blocks (Day7: p=0.0135; Day9: p=0.0489). The *FE65*$^{+/-}$ mice did not differ from either the *FE65*$^{+/+}$ mice or the *FE65*$^{-/-}$ mice, given the assumption that they should exhibit an intermediate behavior. Analysis of platform searching patterns did not reveal significant differences in thigmotaxis among genotypes (data not shown). These data indicated that *FE65*$^{-/-}$ mice were competent on procedural components of the hidden platform version of MWM task and could remember the spatial cues necessary to solve the task, although not as efficiently as *FE65*$^{+/+}$ mice.

Reversal Test:

The mice were further tested during an additional three-day period of reversal training in order to determine the efficiencies with which they could extinguish memories of the old platform locations and learn the new locations. On the first day of reversal

learning, *FE65*$^{+/+}$ and *FE65*$^{-/-}$ mice exhibited comparable latencies. However, the *FE65*$^{-/-}$ mice failed to improve on subsequent days and showed significantly higher latencies than *FE65*$^{+/+}$ mice from the second day of spatial training (Fig. 4.4 B.). Analysis of reversal results by two-way ANOVA indicated that the groups differed in their average latencies over the 3-day period ($F_{2,24}$=9.19, p=0.0011). ANOVA also revealed major effects of days ($F_{2,48}$=26.54, p<0.0001) and of interaction ($F_{4,48}$=7.79, p=0.0001) indicating that the groups differed in their learning rates. ANOVA of data from the *FE65*$^{-/-}$ group indicated that these mice did not improve their performance over the three days of training ($F_{2,24}$=0.05, p=0.9470). By contrast, *FE65*$^{+/+}$ mice showed significant differences in reversal latencies over the 3-day period of evaluation ($F_{2,27}$=11.93, p=0.0002). Post-hoc analyses demonstrated that the *FE65*$^{-/-}$ group had significantly longer latencies than the control group on reversal days 2 and 3 (p=0.0135; p=0.0002, respectively). *FE65*$^{+/-}$ and *FE65*$^{+/+}$ did not differ from each other. The data from these reversal trials thus indicated that *FE65*$^{-/-}$ mice did not learn the new platform location whereas *FE65*$^{+/-}$ and *FE65*$^{+/+}$ mice did exhibit learning.

Probe Tests:

Probe tests were conducted to assess the retention of spatial information in mice. Analyses of the measurements from probe trials conducted one day after the completion of hidden platform acquisition demonstrated the acquisition of this water maze task for all the groups of mice (Fig. 4.5 A.). All three groups spent significantly more time over the targeted quadrant as compared with other quadrants (ANOVA, F

$_{3,88}$=15.93, p<0.0001). The *FE65*$^{-/-}$ mice also displayed selective search for the missing platform but spent less time than *FE65*$^{+/+}$ controls in the train quadrant (Fig. 4.5 A.). The differences of time in target quadrant and the number of target crossings between *FE65*$^{-/-}$ and *FE65*$^{+/+}$ mice were marginally insignificant (p=0.0709; p=0.0799 respectively).

A probe trial was conducted one day after the completion of reversal training. These reversal probe trials showed that the time spent searching in the training quadrant were significantly different among the different genotypes (Fig. 4.5 B; ANOVA, $F_{2,24}$=10.93, p=0.0004). *FE65*$^{-/-}$ mice spent significantly less time searching in the trained quadrant than did *FE65*$^{+/+}$ mice (7.44 sec vs. 22.08 sec; p= 0.0002), confirming that the *FE65*$^{-/-}$ mice have impaired reversal spatial learning. Interestingly, whereas the *FE65*$^{+/+}$ mice searched selectively for the missing platform in the training quadrant, the *FE65*$^{-/-}$ mice persisted in searching the opposite quadrant where the platform has been previously located. The time spent in the opposite quadrant was significantly longer compared with *FE65*$^{+/+}$ mice (*FE65*$^{+/+}$ 10.2 sec vs. *FE65*$^{-/-}$ 19.8 sec; p=0.0372). *FE65*$^{+/-}$ mice, however, spent as much time as *FE65*$^{+/+}$ mice in the training quadrant (p>0.05) but significantly longer time than *FE65*$^{-/-}$ mice (p=0.0152). The numbers of target crossings for the *FE65*$^{-/-}$ group, but not for the *FE65*$^{+/-}$group, were also significantly less as compared to *FE65*$^{+/+}$ mice (Fig. 4.5 B; p=0.0004). These data indicated that *FE65*$^{-/-}$ mice retain a spatial preference that is no longer

appropriate; these *FE65* knockout mice, therefore, are deficient in learning new spatial information.

Visible Platform Acquisition

The visible platform version of the MWM was used to test non-spatial learning and to assess whether spatial learning deficits detected in $FE65^{-/-}$ mice were a result of deficient escape motivation or impairment of visual and/or motor performance. All groups of mice had no difficulties in locating the platform and climbing onto it. There therefore were no detectable differences in motor performance. An ANOVA revealed that all groups of mice improved their performances as measured by decreases of escape latencies over the training days (Fig. 4.4 D. $F_{2,24}=10.93$, $p>0.05$). The differences between groups were not significant ($F_{2,24}=19.9$, $p>0.05$). There were no significant genotype × day interactions.

Swimming Speeds

Swimming speeds were also analyzed to determine whether the groups differed in swimming abilities. ANOVA of these data yielded no significant differences between genotypes on the hidden platform trials (Fig. 4.4 C.), suggesting that sensorimotor disturbances or other non-associative factors were not differentially affecting group performance.

4.4. Discussion

Despite the fact that we only succeeded in a knockout of the full-length isoform, behavioral analyses revealed remarkably strong deficits in hippocampal dependent learning and memory in the mutant animals. p97FE65$^{-/-}$ mice exhibited slow acquisition rates on both aversive and spatial memory tasks, and severe impairments in spatial memory extinction during relearning, after exclusion of potential confounding decrements of locomotor activity, visual acuity, and pain perception in mutant mice. p97FE65$^{+/-}$ mice showed intermediate phenotypes somewhere between *FE65* wild type and p97FE65$^{-/-}$ in most of these tests except for the MWM reversal-learning test, reflecting gene-does-dependent effects. The most dramatic finding in the present study was that p97FE65$^{-/-}$ mice were severely impaired in the reversal-learning test. In contrast to the learning of the first spatial preference, where these mice only exhibited slightly reduced ability, the impairments in reversal learning were so profound that the escape latencies of these mice were kept unchanged over the 3-day tested period (Fig. 4.4 B). The failure of these mice to relearn the new spatial preference may be due to inappropriate perseverance of their originally trained preference (Fig. 4.5 B), suggesting that the mice may have deficits in spatial memory extinction, a process associated with active suppression of original association and the re-establishment of a new one, rather than simple memory decay (Abel and Lattal, 2001). Interestingly, this particular phenotype appears to be recessive, suggesting that the presence of minimum amounts of FE65 proteins (e.g. p97) may be essential for

maintaining this function. Similarly impaired memory-extinction phenotypes have also been found in the mutant mice with knocked out CB1 cannabinoid receptor (Varvel et al., 2002), a retrograde modulator of synaptic activities at the presynaptic membrane (Wilson and Nicoll, 2002).

In contrast to spatial acquisition, which mainly depends on the function of the hippocampus, the mutant mice also showed severe impairments in aversive learning assessed by passive avoidance, a measurement that is mediated by amygdala and striatal structures, in addition to the hippocampus (Picciotto and Wickman 1998), suggesting that FE65 may function in several brain regions. The observed behavioral phenotypes are consistent with expression patterns of FE65 in brain. Abundant FE65 has been found in cerebral cortex, the CA1 and CA3 regions of hippocampus, the basolateral nucleus of amygdala, and striatum (Bressler et al., 1996; Kesavapany et al., 2002). Although *FE65* is highly expressed in the cerebellum, cerebellar associated functions, e.g. locomotor activity, were not impaired in the mutant mice.

Our experiments revealed interesting effects of aging. Older wild type mice showed significantly reduced learning and memory capacity than their younger cohorts, which was as expected, whereas the performance of p97FE65$^{-/-}$ mice at advanced age was not significantly changed (Fig. 4.3 A.). There was in fact some evidence of slightly better performance of p97FE65$^{-/-}$ mice at age of 27 months than their wild type cohorts, although the difference did not reach statistical significance. These results

suggest that FE65 may enhance learning and memory during the early stages of life, but might have deleterious effects on memory late in the life span. Put differently, lack of or reduced FE65 function may produce sub-optimal memory early in life but may have protective effects late in life. Consistent with this idea, we had previously found that the major polymorphic allele of human *FE65*, an allele that first appears in *Homo sapiens,* codes for an FE65 protein that provides a very strong interaction with βPP (Hu et al., 2002). We speculated that this allele might have been selected for enhanced cognitive functions. That allele, however, was shown to be a risk factor for very late onset dementias of the Alzheimer type (VLODAT) (Hu et al., 2002). The minor *FE65* allele, carried by only approximately 25% of Northern European/North American Caucasian populations, resembles the alleles in other species in that it codes for an FE65 protein that exhibits only weak βPP binding. Human subjects carrying that allele are relatively resistant to VLODAT. Therefore, FE65 may function differently in different phases of the life span.

It is not clear whether the phenotype we have observed in the mutant mice is due to loss of p97, to increased expression of p60, or to both. Complete loss of p97, however, may have more impact upon cellular functions than the increased expression of p60 resulting from our partial knockout. We believe that loss of the full-length FE65 function may be a more plausible explanation of the observed phenotype in mutant mice. This hypothesis is supported by the recessive trait of the severely impaired reversal learning of mutant mice at age of 14 months (Fig. 4.4 B). A fuller

understanding of *FE65* gene action will require the generation of mice with a complete deletion of *FE65* gene expression as well as mice incapable of expressing p60.

We have conducted behavioral tests on mice at middle (14 months) and old ages (27 months). It would be informative to carry out tests at ages within 2-12 months range in order to establish the onset of cognitive impairment in each of the testing paradigms used. Our western results of FE65 expressions during development and aging showed that FE65 levels peak at 3 months old. Therefore, FE65 mutant mice may have developed the cognitive deficits at younger ages. The developmental progression of the cognitive impairment should be addressed for the FE65 mutant mice in the future. It would also be interesting to determince whether other forms and phases of memory function, such as short-term memory, memory consolidation and retention, are intact in our FE65 mutant mice.

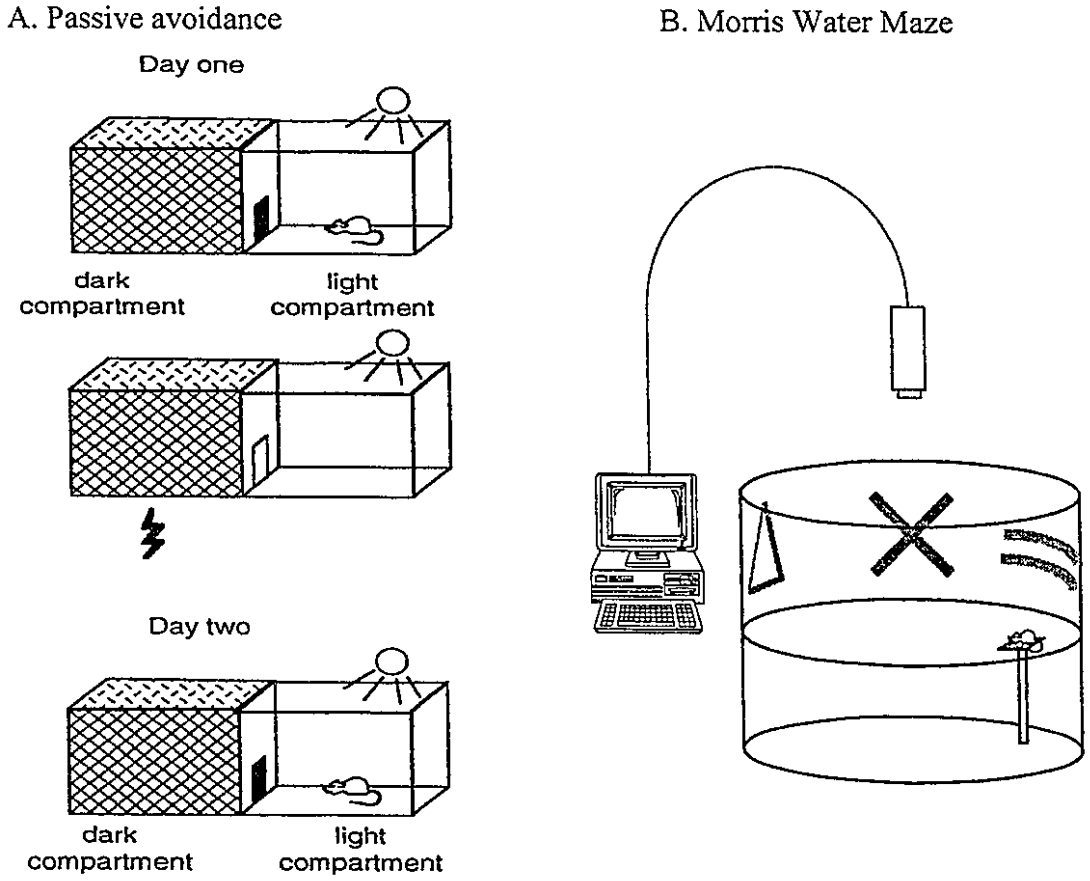

(Physiological Reviews Vol.78, No.4,1998)

Figure 4.1. Common learning tests. **A.** Passive avoidance apparatus and procedure for testing associative aversive memory. On day1, the animal is allowed to explore the apparatus. Once it enters the dark chamber, a foot shock is administered. Twenty-four hours later, the latency time to reenter the dark chamber is measured. **B.** Morris water maze. The animal is placed in water and learns to use 3-dimensional cues to find a platform hidden beneath the surface of water. After several training trials, animal leans to find the platform. Memory can also be tested by removing the platform and measuring the amount of time the animal spends exploring the quadrant that had contained the platform, or the number of times the animal crossed to the quadrant that contained the platform. Controls for physical abnormalities and deficits in nonspatial learning are carried out by assessing performance in finding a visible platform marked by a flag.

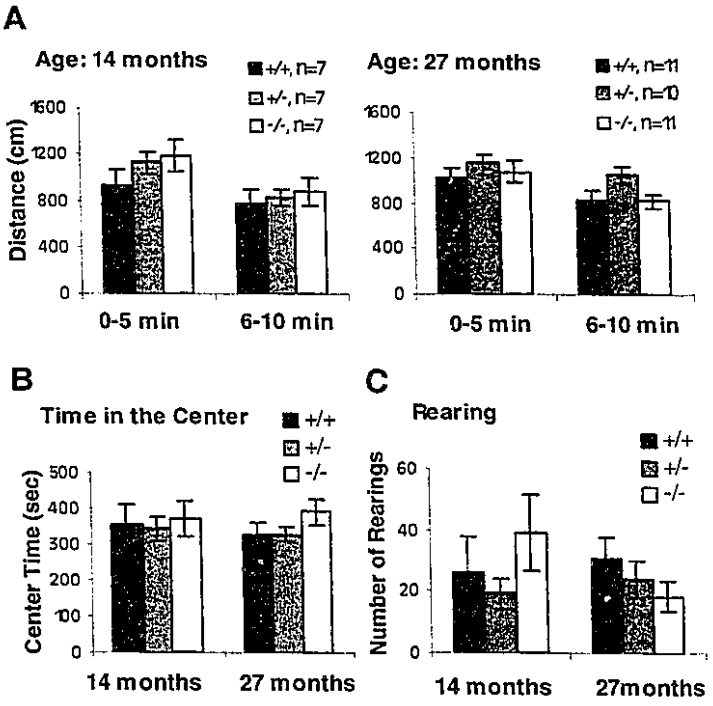

Figure 4.2. Measures of locomotor activity and open field behavior. **A.** Distance traveled in the open field arena was recorded over 10 min; results were separately analyzed for the periods of 0-5 and 6-10 min, expressed as means ± SEM. At 14 months of age (left panel) and at 27 months of age (right panel), no differences were found in the total distances traveled among genotypes (*FE65*$^{+/+}$, *FE65*$^{+/-}$ and *FE65*$^{-/-}$). **B.** The time spent in the central portions of the open field apparatus (Central Time) revealed no differences among genotypes at both ages. **C.** The number of episodes of rearing (vertical beam breaks) were not significantly different among genotypes at both ages.

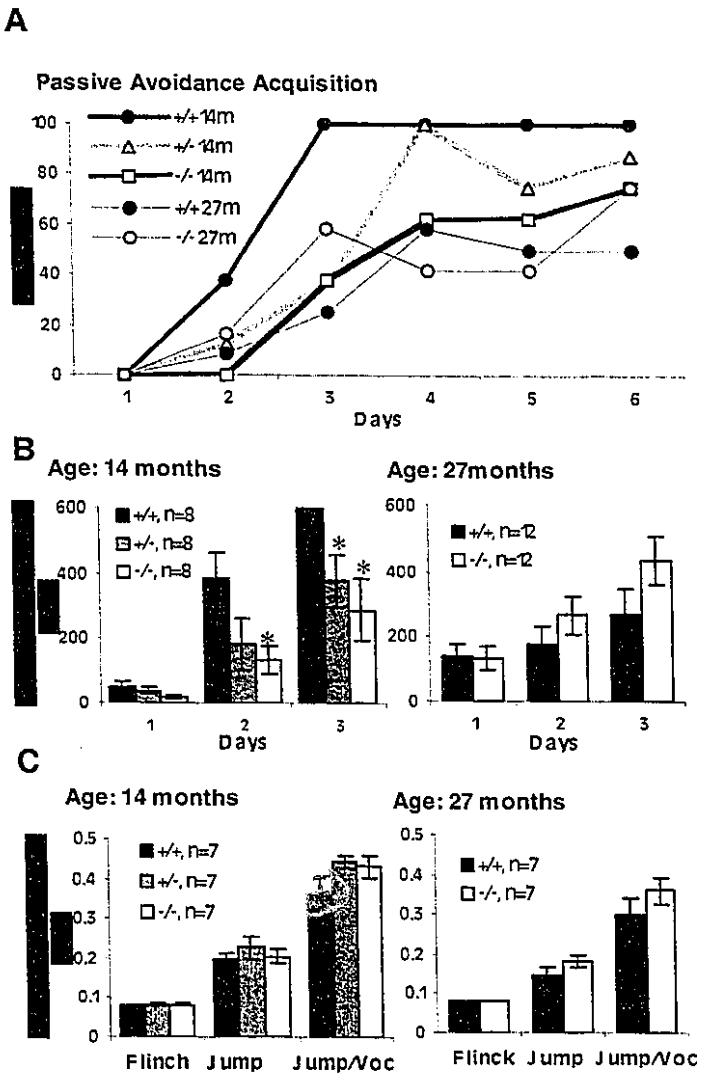

Figure 4.3. Performance of FE65 mutant mice in a passive avoidance test. **A.** The percentage of mice that completely avoided the dark compartment (reached 600 sec step-through latency) in each day was plotted. *FE65*$^{+/-}$ and *FE65*$^{-/-}$ mice at 14 months of age showed depressed learning curves when compared with *FE65*$^{+/+}$ mice. At 27 months of age, the performances of *FE65*$^{+/+}$ and *FE65*$^{-/-}$ mice were comparable to each other and similar to *FE65*$^{-/-}$ mice at 14 months of age. **B.** At 14 months of age (left panel), the step-through latencies of *FE65*$^{+/-}$ and *FE65*$^{-/-}$ mice were significantly shorter as compared to those of *FE65*$^{+/+}$ mice on days 2 and 3 (*p<0.05; **p<0.001). At 27 months of age (right panel), the differences of step through latencies between *FE65*$^{+/+}$ and *FE65*$^{-/-}$ mice were not significant. **C.** Shock thresholds for vocalization and jumping were not significantly different among groups at 14 months (left panel) and 27 months old (right panel).

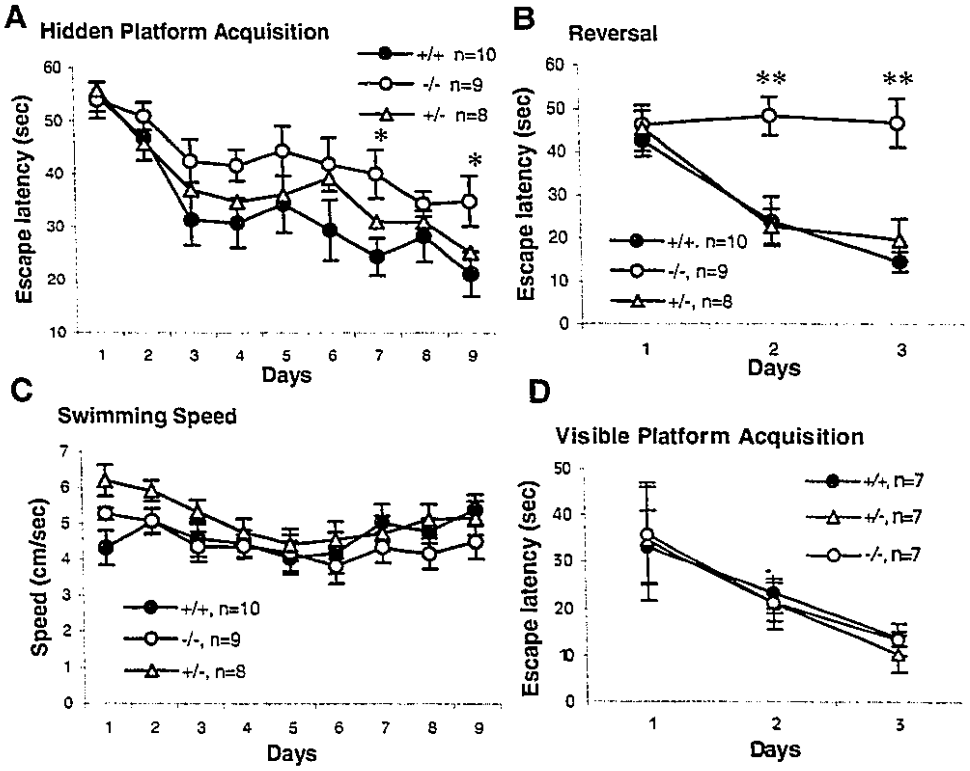

Figure 4.4. Performance of FE65 mutant mice in the Morris water maze. **A.** Acquisition of hidden platform locations. The groups were found to differ significantly on the hidden platform trials in terms of escape latencies during the 7th and 9th days (*p<0.05). **B.** Reversal learning test. *FE65*$^{-/-}$ animals differed significantly from *FE65*$^{+/-}$ and *FE65*$^{+/+}$ mice on reversal days 2 and 3 (**p<0.0002). **C.** Speed of swimming in the hidden-platform test. No significant differences were observed among the genotypes. **D.** Acquisition of visible platform locations. No significant effects of genotypes were observed.

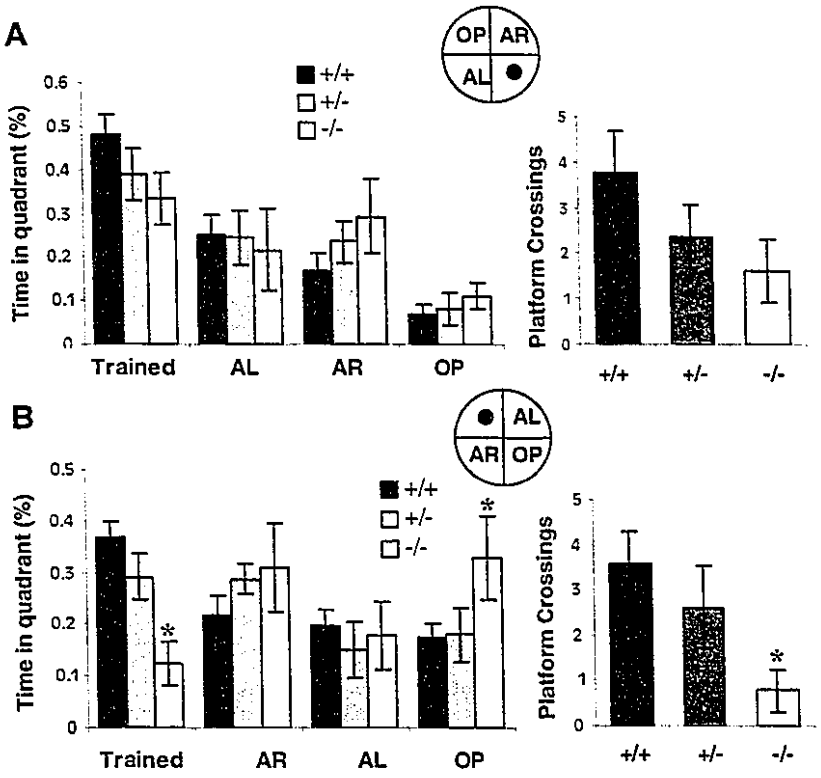

Figure 4.5. Performance of FE65 mutant mice in probe tests. **A.** Probe test performed one day after the hidden platform acquisition period. Percentage time spent in each of four quadrants (left panel) and the number of target crossing (right panel) revealed that *FE65*$^{-/-}$ mice spent shorter times in the trained quadrant and had fewer target crossings than *FE65*$^{-/-}$ mice. The differences were marginally insignificant (p=0.07). **B.** Probe test performed one day after the reversal period. *FE65*$^{+/+}$ mice spent more time searching in the trained quadrant, whereas *FE65*$^{-/-}$ mice did not exhibit this preference. *FE65*$^{-/-}$ mice persisted in searching in the opposite quadrant, where the platform was formerly located (left panel; *p<0.002). The number of target crossings for *FE65*$^{-/-}$ mice was significantly less as compared with *FE65*$^{+/+}$ mice (right panel; *p<0.05).

CHAPTER 5

CONCLUSIONS AND FUTURE DIRECTIONS

5.1. Conclusions and Implications:

We generated a line of *FE65* knockout mice by a well-established gene targeting methodology and documented that these mice do not express full-length FE65 mRNAs and proteins. However, a novel truncated isoform of FE65 (p60) was expressed. These mice were viable, fertile, and apparently normal as regards gross and light microscopic anatomy, locomotor activity, visual acuity, and pain perception when compared with their wild type cohorts. Despite the upregulated expression of p60 in mutant mice, the homozygous *FE65* mutants exhibited slower acquisition rates of both aversive and spatial memory tasks and exhibited robust impairments in spatial memory extinction during re-learning. These results suggest that one of the primary physiological functions of FE65 may involve learning and memory processing in the hippocampus.

Although the molecular mechanisms whereby FE65 contribute to normal and altered hippocampal dependent learning and memory are not clear, its interaction with βPP and its role as an adaptor or scaffold protein within the broader network of associated proteins are likely to be of major significance. Supporting evidence comes from our

results showing that secretion of Aβ peptides in the media of primary neuronal cultures derived from p97FE65$^{-/-}$/Tg2576 mice is decreased. This finding might seem puzzling, given the fact that p60, which has an intact βPP binding domain, is preserved in the FE65 mutant mice. It could also imply that the N-terminus of p97 might be critical to the modulation of βPP trafficking and processing. In fact, our results are consistent with previous reports that overexpression of the full-length FE65 increases secretion of Aβ peptides (Sabo et al., 1999). A large body of evidence has implicated Aβ peptides as central to the pathogenesis of Alzheimer disease. However, the functional relationship of βPP and its proteolyticly cleaved products to learning and memory is not known. Aβ peptides are generated in physiological conditions, suggesting that they may have unique functions in brain. There is increasing evidence supporting a role of Aβ in mediating synaptic functions. Recent observations have indicated that neuronal activity can modulate βPP processing and endogenous Aβ production; Aβ in turn may provide negative feedback on neuronal function (Kamenetz et al., 2003). The decreased levels of Aβ associated with our *FE65* mutant mice might therefore reflect a disrupted feedback system on neuronal activity, thus contributing to the cognitive deficits we have observed in such mice. The level of AICD peptides (peptides representing the β-amyloid precursor protein intracellular domain), another product of βPP processing, may also be affected by deficiencies in FE65, given published evidence that FE65 can stabilize AICD (Kimberly et al. 2001, Zheng et al., 2002). There is emerging evidence of a role of AICD in important

nuclear signaling events (Cao and Sudhof 2001; Gao et al., 2001) and in modulation of calcium signaling (Leissring et al., 2002), a process important to synaptic plasticity. We therefore propose that FE65 plays crucial roles in the release and subsequent signaling of βPP fragments, such as Aβ and AICD, and that alterations in these processes may explain the cognitive alterations we have observed in our knockout mice.

Mice with interrupted expression of *βPP* were impaired in spatial learning and exploratory behavior (Muller at al., 1994). Forebrain-conditional *PS1* knockout mice exhibit memory clearance deficits (Feng et al., 2001), which are to some extent similar to the memory extinction deficits we have observed in p97FE65$^{-/-}$ mice. Mutations in *βPP* and *PS1* contribute to a large portion of early onset dementias of the Alzheimer type (for review, see Selkoe 2001). A minor polymorphism in human *FE65* is found to associate with resistance to very late onset dementias of the Alzheimer type by generation of a splicing isoform with altered affinity to AICD (Hu et al., 2002; Lambert et al., 2000). Thus, it is likely that each major component of the PS1-βPP-FE65 signaling pathway contributes to the cognitive "fitness" of mammalian organisms during the early stages of their life spans. We speculate, however, that, given highly active robust functions, a "price may be paid" – deleterious functioning late in the life span (Hu et al., 2002, Fig. 5.1).

5.2. Future Directions:

5.2.1. Gene Expression Profiling by Microarray and Quantitative RT-PCR

Since FE65 has been implicated in the regulation of gene transcription (Cao and Sudhof, 2001), it will be of interest to survey the genes that were upregulated or downregulated in the FE65 mutant mice by Microarray and Quantitative RT-PCR. These studies may enable us to reveal novel biochemical pathways and functional interactions between FE65 and other genes.

5.2.2. Role of FE65 in Synaptic Plasticity

Synaptic plasticity is generally believed to be a major candidate neural mechanism for learning and memory (Kandel., 2001). It is important to pursue electrophysiological studies on the FE65 mutant mice to correlate impaired synaptic plasticity with cognitive deficits seen in these mice. These studies will not only validate the phenotype but also will significantly strengthen the favored interpretation of cognitive fitness associated with the level of FE65 protein. Measurements of the long- term potentiation (LTP) using brain hippocampal slices from FE65 mutant mice are now being carried out by a senior postdoctoral fellow in the laboratory of Dr. Dan Storm. Preliminary results show that the FE65 mutant mice have LTP deficits (H. Wang).

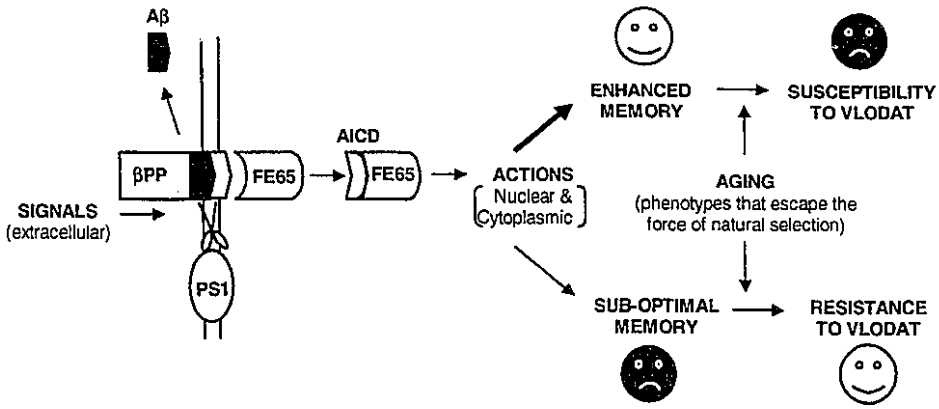

Figure 5.1. A simplified model of gene actions involving a segment of the FE65 protein network. The γ-secretase cut (mediated by PS1 and co-factors) serves as the "RIP" (Brown et al., 2000) for the liberation of AICD (βPP intracellular domain), which interact with FE65 to modulate cytoplasmic and nuclear functions relevant for memory during the earlier stages of the life course (those susceptible to the force of natural selection). The predominant *FE65* allele is thought to have evolved as part of a suite of gene actions leading to enhanced cognitive functions. During the latter half of the life span, however, relatively strong activities of this pathway may contribute to the development of early onset DAT (e.g., in families with mutations in *PS1* and *APP* genes) or may be associated with increased susceptibility to very late onset case of DAT (e.g., for the case of allele 1 of *FE65*).

References:

Abel T, Lattal KM (2001) Molecular mechanisms of memory acquisition, consolidation and retrieval. Curr Opin Neurobiol 11(2):180-187.

Ando K, Iijima KI, Elliott JI, Kirino Y, Suzuki T (2001) Phosphorylation-dependent regulation of the interaction of amyloid precursor protein with Fe65 affects the production of beta-amyloid. J Biol Chem 276(43):40353-40361.

Angrini M, Leslie JC, Shephard RA (1998) Effects of propranolol, buspirone, pCPA, reserpine, and chlordiazepoxide on open-field behavior. Pharmacol Biochem Behav 59:387-397.

Annaert W, De Strooper B (1999) Presenilins: molecular switches between proteolysis and signal transduction. Trends Neurosci 22(10):439-443.

Baek SH, Ohgi KA, Rose DW, Koo EH, Glass CK, Rosenfeld MG (2002) Exchange of N-CoR corepressor and Tip60 coactivator complexes links gene expression by NF-kappaB and beta-amyloid precursor protein. Cell. 110(1):55-67.

Banker G, Goslin K. Culturing nerve cells. Cambridge, Mass.: MIT Press, c1998.

Berman DE, Dudai Y (2001) Memory extinction, learning anew, and learning the new: dissociations in the molecular machinery of learning in cortex. Science 23;291(5512):2417-2419.

Blaikie P, Immanuel D, Wu J, Li N, Yajnik V, Margolis B (1994) A region in Shc distinct from the SH2 domain can bind tyrosine-phosphorylated growth factor receptors. J Biol Chem. 269(51):32031-4.

Borg JP, Ooi J, Levy E, Margolis B (1996) The phosphotyrosine interaction domains of X11 and FE65 bind to distinct sites on the YENPTY motif of amyloid precursor protein. Mol Cell Biol 16(11):6229-6241.

Bork, P., and Sudol, M. The WW domain: a signalling site in dystrophin? 1994 Trends. Biochem. Sci. 19:531-533.

Bork P, Margolis B. A phosphotyrosine interaction domain. 1995 Cell. Mar 10;80(5):693-4.

Bressler SL, Gray MD, Sopher BL, Hu Q, Hearn MG, Pham DG, Dinulos MB, Fukuchi K, Sisodia SS, Miller MA, Disteche CM, Martin GM (1996) cDNA cloning and chromosome mapping of the human Fe65 gene: interaction of the conserved cytoplasmic domains of the human beta-amyloid precursor protein and its homologues with the mouse Fe65 protein. Hum Mol Genet 5(10):1589-1598.

Brouillet E, Trembleau A, Galanaud D, Volovitch M, Bouillot C, Valenza C, Prochiantz A, Allinquant B. The amyloid precursor protein interacts with Go heterotrimeric protein within a cell compartment specialized in signal transduction. J Neurosci. 1999 Mar 1;19(5):1717-27.

Brown MS, Ye J, Rawson RB, Goldstein JL (2000) Regulated intramembrane proteolysis: a control mechanism conserved from bacteria to humans. Cell.100(4):391-398.

Bruni P, Minopoli G, Brancaccio T, Napolitano M, Faraonio R, Zambrano N, Hansen U, Russo T. (2002) Fe65, a ligand of the Alzheimer's beta-amyloid precursor protein, blocks cell cycle progression by down-regulating thymidylate synthase expression.

Buxbaum JD, Liu KN, Luo Y, Slack JL, Stocking KL, Peschon JJ, Johnson RS, Castner BJ, Cerretti DP, Black RA. (1998) Evidence that tumor necrosis factor alpha converting enzyme is involved in regulated alpha-secretase cleavage of the Alzheimer amyloid protein precursor. J Biol Chem. 273(43):27765-7.

Cai H, Wang Y, McCarthy D, Wen H, Borchelt DR, Price DL, Wong PC. BACE1 is the major beta-secretase for generation of Abeta peptides by neurons. Nat Neurosci. 2001 Mar;4(3):233-234

Cao X., and Südhof TC (2001) A transcriptionally active complex of APP with Fe65 and histone acetyltransferase Tip60. Science 293, 115-120.

Carlson GA, Borchelt DR, Dake A, Turner S, Danielson V, Coffin JD, Eckman C, Meiners J, Nilsen SP, Younkin SG, Hsiao KK (1997) Genetic modification of the phenotypes produced by amyloid precursor protein overexpression in transgenic mice. Hum Mol Genet. 6(11):1951-1959.

Chapman PF, White GL, Jones MW, Cooper-Blacketer D, Marshall VJ, Irizarry M, Younkin L, Good MA, Bliss TV, Hyman BT, Younkin SG, Hsiao KK. (1999) Impaired synaptic plasticity and learning in aged amyloid precursor protein transgenic mice. Nat Neurosci 2(3):271-276.

Chen Y, McPhie DL, Hirschberg J, Neve RL. The amyloid precursor protein-binding protein APP-BP1 drives the cell cycle through the S-M checkpoint and causes apoptosis in neurons. J Biol Chem 2000 Mar 24;275(12):8929-35

Chow N, Korenberg JR, Chen XN, Neve RL. APP-BP1, a novel protein that binds to the carboxyl-terminal region of the amyloid precursor protein. J Biol Chem. 1996 May 10;271(19):11339-46.

Cornelis S, Bruynooghe Y, Denecker G, Van Huffel S, Tinton S, Beyaert R. (2000) Identification and characterization of a novel cell cycle-regulated internal ribosome entry site. Mol Cell. 5(4):597-605.

Crawley JN, Paylor R (1997) A proposed test battery and constellations of specific behavioral paradigms to investigate the behavioral phenotypes of transgenic and knockout mice. Horm Behav 31(3):197-211.

Crusio WE, Schwegler H, van Abeelen JH (1989) Behavioral responses to novelty and structural variation of the hippocampus in mice. I. Quantitative-genetic analysis of behavior in the open-field. Behav Brain Res 32(1):75-80.

Cupers P, Orlans I, Craessaerts K, Annaert W, De Strooper B (2001) The amyloid precursor protein (APP)-cytoplasmic fragment generated by gamma-secretase is rapidly degraded but distributes partially in a nuclear fraction of neurones in culture.

Davis CG, Lehrman MA, Russell DW, Anderson RG, Brown MS, Goldstein JL (1986) The J.D. mutation in familial hypercholesterolemia: amino acid substitution in cytoplasmic domain impedes internalization of LDL receptors. Cell. 45(1):15-24

Dawson GR, Seabrook GR, Zheng H, Smith DW, Graham S, O'Dowd G, Bowery BJ, Boyce S, Trumbauer ME, Chen HY, Van der Ploeg LH, Sirinathsinghji DJ. Age-related cognitive deficits, impaired long-term potentiation and reduction in synaptic marker density in mice lacking the beta-amyloid precursor protein. Neuroscience. 1999 Apr;90(1):1-13.

De Strooper B, Annaert W. Proteolytic processing and cell biological functions of the amyloid precursor protein. J Cell Sci. 2000 Jun;113 (Pt 11):1857-70.

De Strooper B, Umans L, Van Leuven F, Van Den Berghe H. Study of the synthesis and secretion of normal and artificial mutants of murine amyloid precursor protein (APP): cleavage of APP occurs in a late compartment of the default secretion pathway. J Cell Biol. 1993 Apr;121(2):295-304.

Duff K, Knight H, Refolo LM, Sanders S, Yu X, Picciano M, Malester B, Hutton M, Adamson J, Goedert M, Burki K, Davies P. Characterization of pathology in transgenic mice over-expressing human genomic and cDNA tau transgenes. Neurobiol Dis. 2000 Apr;7(2):87-98.

Duilio A, Faraonio R, Minopoli G, Zambrano N, Russo T (1998) Fe65L2: a new member of the Fe65 protein family interacting with the intracellular domain of the Alzheimer's beta-amyloid precursor protein. Biochem J 330 (Pt 1):513-519.

Duilio A, Zambrano N, Mogavero AR, Ammendola R, Cimino F, Russo T (1991) A rat brain mRNA encoding a transcriptional activator homologous to the DNA binding domain of retroviral integrases. Nucleic Acids Res 19(19):5269-5274.

Dyer JR, Michel S, Lee W, Castellucci VF, Wayne NL, Sossin WS (2003) An activity-dependent switch to cap-independent translation triggered by eIF4E dephosphorylation. Nat Neurosci. 6(3):219-220.

Ermekova KS, Zambrano N, Linn H, Minopoli G, Gertler F, Russo T, Sudol M (1997) The WW domain of neural protein FE65 interacts with proline-rich motifs in Mena, the mammalian homolog of Drosophila enabled. J Biol Chem 272(52):32869-32877.

Esch, F.S., Keim, P.S., Beattie, E.C., Blacher, R.W., Culwell, A.R., Oltersdorf, T., McClure, D., and Ward P.J. Cleavage of amyloid beta peptide during constitutive processing of its precursor, 1990 Science 248:1122-1124.

Esler, WP, Kimberly, WT, Ostaszewski, BL, Ye, W, Diehl, TS, Selkoe, DJ & Wolfe, MS. (2002) Activity-dependent isolation of the presenilin- ?-secretase complex reveals nicastrin and a ? substrate. Proc. Natl. Acad. Sci. USA 99, 2720-2725.

Faraonio R, Minopoli G, Porcellini A, Costanzo F, Cimino F, Russo T. The DNA sequence encompassing the transcription start site of a TATA-less promoter contains information to drive neuron-specific transcription. Nucleic Acids Res. 1994 Nov 25;22(23):4876-83.

Feng R, Rampon C, Tang YP, Shrom D, Jin J, Kyin M, Sopher B, Miller MW, Ware CB, Martin GM, Kim SH, Langdon RB, Sisodia SS, Tsien JZ (2001) Deficient neurogenesis in forebrain-specific presenilin-1 knockout mice is associated with reduced clearance of hippocampal memory traces. Neuron 32(5):911-926.

Fiore F, Zambrano N, Minopoli G, Donini V, Duilio A, Russo T (1995) The regions of the Fe65 protein homologous to the phosphotyrosine interaction/phosphotyrosine binding domain of Shc bind the intracellular domain of the Alzheimer's amyloid precursor protein. J Biol Chem 270(52):30853-30856.

Frohman, M.A., Dush, M.K., and Martin, G.R. Rapid production of full-length cDNAs from rare transcripts: amplification using a single gene-specific oligonucleotide primer. 1988 Proc. Natl. Acad. Sci. U.S.A. 85, 8998-9002.

Games, D., Adams, D., Alessandrini, R., Barbour, R., Berthelette, P., Blackwell, C., Carr, T., Clemens, J., Donaldson, T., Gillespie, F. and et al. Alzheimer-type neuropathology in transgenic mice overexpressing V717F beta-amyloid precursor protein. 1995 Nature 373:523-527

Gao Y, Pimplikar SW (2001) The gamma -secretase-cleaved C-terminal fragment of amyloid precursor protein mediates signaling to the nucleus. Proc Natl Acad Sci U S A 98(26):14979-14984.

Gerlai R (2001) Gene targeting: technical confounds and potential solutions in behavioral brain research. Behav Brain Res. 125(1-2):13-21.

Gertler FB, Niebuhr K, Reinhard M, Wehland J, Soriano P. Mena, a relative of VASP and Drosophila Enabled, is implicated in the control of microfilament dynamics. Cell. 1996 Oct 18;87(2):227-39.

Goate A, Chartier-Harlin MC, Mullan M, Brown J, Crawford F, Fidani L, Giuffra L, Haynes A, Irving N, James L, Mant R, Newton P, Rooke K, Roques P,Talbot C, Pericak_Vance M, Roses A, Williamson R, Rossor M, Owen M, Hardy J. Segregation of a missense mutation in the amyloid precursor protein gene with familial Alzheimer's disease. Nature. 1991 Feb 21;349(6311):704-6.

Guenette SY, Chen J, Ferland A, Haass C, Capell A, Tanzi RE (1999) hFE65L influences amyloid precursor protein maturation and secretion. J Neurochem 73(3):985-993.

Guenette SY, Chen J, Jondro PD, Tanzi RE (1996) Association of a novel human FE65-like protein with the cytoplasmic domain of the beta-amyloid precursor protein. Proc Natl Acad Sci U S A 93(20):10832-10837.

Guenette SY, Bertram L, Crystal A, Bakondi B, Hyman BT, Rebeck GW, Tanzi RE, Blacker D. Evidence against association of the FE65 gene (APBB1) intron 13 polymorphism in Alzheimer's patients. Neurosci Lett. 2000 Dec 15;296(1):17-20.

Haass, C. and Selkoe, D.J. Cellular processing of ?-amyloid precursor protein and the genesis of amyloid ?-peptide. 1993 Cell 75: 1039-104.

Hardy J. The Alzheimer family of diseases: many etiologies, one pathogenesis? Proc Natl Acad Sci U S A. 1997 Mar 18;94(6):2095-7.

He W, O'Neill TJ, Gustafson TA (1995) Distinct modes of interaction of SHC and insulin receptor substrate-1 with the insulin receptor NPEY region via non-SH2 domains. J Biol Chem. 270(40):23258-62.

He Y, Armanious MK, Thomas MJ, Cress WD. Identification of E2F-3B, an alternative form of E2F-3 lacking a conserved N-terminal region. 2000 Oncogene 19, 3422-3433.

Holcik M, Sonenberg N, Korneluk RG (2000) Internal ribosome initiation of translation and the control of cell death. Trends Genet. 16(10):469-473.

Homayouni R, Rice DS, Sheldon M, Curran T. Disabled-1 binds to the cytoplasmic domain of amyloid precursor-like protein 1. J Neurosci. 1999 Sep 1;19(17):7507-15.

Hsiao KK, Borchelt DR, Olson K, Johannsdottir R, Kitt C, Yunis W, Xu S, Eckman C, Younkin S, Price D, Iadecola C, Clark HB, Carlson G (1995) Age-related CNS disorder and early death in transgenic FVB/N mice overexpressing Alzheimer amyloid precursor proteins. Neuron.15(5):1203-1218.

Hsiao K, Chapman P, Nilsen S, Eckman C, Harigaya Y, Younkin S, Yang F, Cole G (1996) Correlative memory deficits, Abeta elevation, and amyloid plaques in transgenic mice. Science 274(5284):99-102.

Hu Q, Hearn MG, Jin LW, Bressler SL, Martin GM. Alternatively spliced isoforms of FE65 serve as neuron-specific and non-neuronal markers. J Neurosci Res. 1999 Dec 1;58(5):632-40.

Hu Q, Kukull WA, Bressler SL, Gray MD, Cam JA, Larson EB, Martin GM, Deeb SS (1998) The human FE65 gene: genomic structure and an intronic biallelic polymorphism associated with sporadic dementia of the Alzheimer type. Hum Genet 103(3):295-303.

Hu Q, Jin LW, Starbuck MY, Martin GM. Broadly altered expression of the mRNA isoforms of FE65, a facilitator of beta amyloidogenesis, in Alzheimer cerebellum and other brain regions. J Neurosci Res. 2000 Apr 1;60(1):73-86.

Hu Q, Cool BH, Wang B, Hearn MG, Martin GM (2002) A candidate molecular mechanism for the association of an intronic polymorphism of FE65 with resistance to very late onset dementia of the Alzheimer type. Hum Mol Genet 11(4):465-475.

Jin LW, Hearn MG, Ogburn CE, Dang N, Nochlin D, Ladiges WC, Martin GM (1998) Transgenic mice over-expressing the C-99 fragment of betaPP with an alpha-secretase site mutation develop a myopathy similar to human inclusion body myositis. Am J Pathol. 153(6):1679-1686.

Kamal A, Stokin GB, Yang Z, Xia CH, Goldstein LS. (2002) Axonal transport of amyloid precursor protein is mediated by direct binding to the kinesin light chain subunit of kinesin-I. Neuron. 28(2):449-459.

Kandel ER. (2001) The molecular biology of memory storage: a dialogue between genes and synapses. Science. 294(5544):1030-1038.

Kang J, Lemaire HG, Unterbeck A, Salbaum JM, Masters CL, Grzeschik KH, Multhaup G, Beyreuther K, Muller-Hill B. (1987) The precursor of Alzheimer disease precursor protein resembles a cell-surface receptor. Nature 325: 733-736.

Kesavapany S, Banner SJ, Lau KF, Shaw CE, Miller CC, Cooper JD, McLoughlin DM (2002) Expression of the Fe65 adapter protein in adult and developing mouse brain. Neuroscience. 115(3):951-960.

Kimberly WT, Zheng JB, Guenette SY, and Selkoe DJ (2001) The intracellular domain of the beta-amyloid precursor protein is stabilized by Fe65 and translocates to the nucleus in a notch-like manner. J Biol Chem 276:40288-40292.

Kim CH, Heath C, Bertuch A, Hansen U. Specific stimulation of simian virus 40 late transcription in vitro by a cellular factor binding the simian virus 40 21-base-pair repeat promoter element. Proc Natl Acad Sci U S A. 1987 Sep;84(17):6025-6029.

Klafki HW, Wiltfang J, Staufenbiel M (1996) Electrophoretic separation of betaA4 peptides (1-40) and (1-42). Anal Biochem 237(1):24-29.

Koo EH, Squazzo SL. Evidence that production and release of amyloid beta-protein involves the endocytic pathway. J Biol Chem. 1994 Jul 1;269(26):17386-9.

Koo EH, Squazzo SL, Selkoe DJ, Koo CH. Trafficking of cell-surface amyloid beta-protein precursor. I. Secretion, endocytosis and recycling as detected by labeled monoclonal antibody. J Cell Sci. 1996 May;109 (Pt 5):991-8.

Koudinov AR, Koudinova NV, Perry G, Smith MA (2002) Alzheimer's disease and amyloid beta protein: dogma is bad for science. Abstract for 32nd annual SFN meeting.

Kozak M. (1996) Interpreting cDNA sequences: some insights from studies on translation. Mammalian Genome 7, 563-574.

Kozak M (2002) Pushing the limits of the scanning mechanism for initiation of translation. Gene. 299(1-2):1-34.

Lai A, Gibson A, Hopkins CR, Trowbridge IS. Signal-dependent trafficking of beta-amyloid precursor protein-transferrin receptor chimeras in madin-darby canine kidney cells. J Biol Chem. 1998 Feb 6;273(6):3732-9.

Lai A, Sisodia SS, Trowbridge IS. Characterization of sorting signals in the beta-amyloid precursor protein cytoplasmic domain. J Biol Chem. 1995 Feb 24;270(8):3565-73.

Lambert JC, Mann D, Goumidi L, Harris,J, Pasquier F, Frigard B, Cottel D, Lendon C, Iwatsubo T, Amouyel P, Chartier-Harlin MC. A FE65 polymorphism associated with risk of developing sporadic late-onset alzheimer's disease but not with Abeta loading in brains. Neurosci Lett. 2000 Oct 20;293(1):29-32.

Lambrechts A, Kwiatkowski AV, Lanier LM, Bear JE, Vandekerckhove J, Ampe C, Gertler FB. cAMP-dependent protein kinase phosphorylation of EVL, a Mena/VASP relative, regulates its interaction with actin and SH3 domains. J Biol Chem. 2000 Nov 17;275(46):36143-51.

Lammich S, Kojro E, Postina R, Gilbert S, Pfeiffer R, Jasionowski M, Haass C, Fahrenholz F. (1999) Constitutive and regulated alpha-secretase cleavage of Alzheimer's amyloid precursor protein by a disintegrin metalloprotease.

Lanier LM, Gates MA, Witke W, Menzies AS, Wehman AM, Macklis JD, Kwiatkowski D, Soriano P, Gertler FB. Mena is required for neurulation and commissure formation. Neuron. 1999 Feb;22(2):313-25.

Lanier LM, Gertler FB. From Abl to actin: Abl tyrosine kinase and associated proteins in growth cone motility. Curr Opin Neurobiol. 2000 Feb;10(1):80-7.

Lau KF, McLoughlin DM, Standen CL, Irving NG, Miller CC. Fe65 and X11beta co-localize with and compete for binding to the amyloid precursor protein. Neuroreport. 2000 Nov 9;11(16):3607-10.

Lau KF, Miller CC, Anderton BH, Shaw PC. Molecular cloning and characterization of the human glycogen synthase kinase-3beta promoter. Genomics. 1999 Sep 1;60(2):121-8.

Launer LJ, Andersen K, Dewey ME, Letenneur L, Ott A, Amaducci LA, Brayne C, Copeland JR, Dartigues JF, Kragh-Sorensen P, Lobo A, Martinez-Lage JM, Stijnen T, Hofman A. Rates and risk factors for dementia and Alzheimer's disease: results from EURODEM pooled analyses. EURODEM Incidence Research Group and Work Groups. European Studies of Dementia. Neurology 1999 Jan 1;52(1):78-84.

Laurent V, Loisel TP, Harbeck B, Wehman A, Grobe L, Jockusch BM, Wehland J, Gertler FB, Carlier MF. Role of proteins of the Ena/VASP family in actin-based motility of Listeria monocytogenes. J Cell Biol. 1999 Mar 22;144(6):1245-58.

LeBlanc AC, Gambetti P. Production of Alzheimer 4kDa beta-amyloid peptide requires the C-terminal cytosolic domain of the amyloid precursor protein. Biochem Biophys Res Commun. 1994 Nov 15;204(3):1371-80.

Leissring MA, Murphy MP, Mead TR, Akbari Y, Sugarman MC, Jannatipour M, Anliker B, Muller U, Saftig P, De Strooper B, Wolfe MS, Golde TE, LaFerla FM (2002) A physiologic signaling role for the gamma -secretase-derived intracellular fragment of APP. Proc Natl Acad Sci U S A 99(7):4697-4702.

Levy-Lahad E, Wasco W, Poorkaj P, Romano DM, Oshima J, Pettingell WH, Yu CE, Jondro PD, Schmidt SD, Wang K, et al. Candidate gene for the chromosome 1 familial Alzheimer's disease locus. Science. 1995 Aug 18;269(5226):973-7.

Lim LC, Swendeman SL, Sheffery M. Molecular cloning of the alpha-globin transcription factor CP2. Mol Cell Biol. 1992 Feb;12(2):828-35.

Liu J, Prolla G, Rostagno A, Chiarle R, Feiner H, Inghirami G. Initiation of translation from a downstream in-frame AUG codon on BRCA1 can generate the novel isoform protein ?BRCA1(17 aa). 2000 Oncogene 19, 2767-2773.

Li YM, Lai MT, Xu M, Huang Q, DiMuzio-Mower J, Sardana MK, Shu XP, Yin KC, Shafer JA, Gardell SJ. Presenilin 1 is linked with ?-secretase activity in the detergent solubilized state. 2000 Proc Natl Acad Sci USA 97: 6138-6143.

Mark MP. Secreted forms of beta-amyloid precursor protein modulate dendrite outgrowth and calcium responses to glutamate in cultured embryonic hippocampal neurons. J Neurobiol. 1994 Apr;25(4):439-50.

Martin GM, Smith AC, Ketterer DJ, Ogburn CE, Disteche CM (1985) Increased chromosomal aberrations in first metaphases of cells isolated from kidneys of aged mice. Isr J Med Sci 21:296-301.

Mattson MP. Cellular actions of ?-amyloid precursor protein and its soluble and fibrillogenic derivatives. Physiological reviews 1997 Oct. Vol 77, No. 4

McLoughlin DM, Miller CC (1996) The intracellular cytoplasmic domain of the Alzheimer's disease amyloid precursor protein interacts with phosphotyrosine-binding domain proteins in the yeast two-hybrid system. FEBS Lett 397(2-3):197-200.

Minopoli G, de Candia P, Bonetti A, Faraonio R, Zambrano N, Russo T (2001) The beta -Amyloid Precursor Protein Functions as a Cytosolic Anchoring Site That Prevents Fe65 Nuclear Translocation. J Biol Chem. 276(9):6545-6550.

Morgan D, Diamond DM, Gottschall PE, Ugen KE, Dickey C, Hardy J, Duff K, Jantzen P, DiCarlo G, Wilcock D, Connor K, Hatcher J, Hope C, Gordon M, Arendash GW (2000) A beta peptide vaccination prevents memory loss in an animal model of Alzheimer's disease. Nature 408(6815):982-985.

Morris, RGM (1982) Place navigation impaired in rats with hippocampal lesions. Nature 297,681-683.

Muller U, Cristina N, Li ZW, Wolfer DP, Lipp HP, Rulicke T, Brandner S, Aguzzi A, Weissmann C (1994) Behavioral and anatomical deficits in mice homozygous for a modified beta-amyloid precursor protein gene. Cell 79(5):755-765.

Nagy A, Rossant J, Nagy R, Abramow-Newerly W, Roder JC (1993) Derivation of completely cell culture-derived mice from early-passage embryonic stem cells. Proc Natl Acad Sci U S A 90(18):8424-8428.

Nishimoto I, Okamoto T, Matsuura Y, Takahashi S, Okamoto T, Murayama Y, Ogata E. Alzheimer amyloid protein precursor complexes with brain GTP-binding protein G(o). Nature. 1993 Mar 4;362(6415):75-9.

Niwa H, Yamamura K, Miyazaki J (1991) Efficient selection for high-expression transfectants with a novel eukaryotic vector. Gene 108:193-199.

Nordstedt, C., Caporaso, G., Thyberg, J., Gandy, S. and Greengard, P. Identification of the Alzheimer ?/A4 amyloid precursor protein in clathrin coated vesicles purified from PC12 cells. 1993 J. Biol.Chem. 268: 608-612

Obermeier A, Bradshaw RA, Seedorf K, Choidas A, Schlessinger J, Ullrich A (1994) Neuronal differentiation signals are controlled by nerve growth factor receptor/Trk binding sites for SHC and PLC gamma. EMBO J. 13(7):1585-90.

Papassotiropoulos A, Bagli M, Becker K, Jessen F, Maier W, Rao ML, Ludwig M, Heun R. No association between an intronic biallelic polymorphism of the FE65 gene and Alzheimer's disease. Int J Mol Med. 2000 Nov;6(5):587-9.

Parvathy S, Karran EH, Turner AJ, Hooper NM. (1998) The secretases that cleave angiotensin converting enzyme and the amyloid precursor protein are distinct from tumour necrosis factor-alpha convertase. FEBS Lett. 1998 Jul 10;431(1):63-5.

Perez RG, Zheng H, Van der Ploeg LH, Koo EH. The beta-amyloid precursor protein of Alzheimer's disease enhances neuron viability and modulates neuronal polarity.
Picciotto MR, Wickman K (1998) Using knockout and transgenic mice to study neurophysiology and behavior. Physiol Rev 78(4):1131-1163.

Picciotto MR, Wickman K (1998) Using deficient and transgenic mice to study neurophysiology and behavior. Physiol Rev 78(4):1131-1163.

Price DL, Tanzi RE, Borchelt DR, Sisodia SS. Alzheimer's disease: genetic studies and transgenic models. Annu Rev Genet. 1998 32:461-93.

Qiu WQ, Ferreira A, Miller C, Koo EH Selkoe DJ. Cell-surface beta-amyloid precursor protein stimulates neurite outgrowth of hippocampal neurons in an isoform-dependent manner. 1995. Journal of Neuroscience, Vol 15, 2157-2167

Ramboz S, Oosting R, Amara DA, Kung HF, Blier P, Mendelsohn M, Mann JJ, Brunner D, Hen R (1998) Serotonin receptor 1A knockout: an animal model of anxiety-related disorder. Proc Natl Acad Sci USA 95:14476-14481.

Roberts CJ, Nelson B, Marton MJ, Stoughton R, Meyer MR, Bennett HA, He YD, Dai H, Walker WL, Hughes TR, Tyers M, Boone C, Friend SH. Signaling and circuitry of multiple MAPK pathways revealed by a matrix of global gene expression profiles. Science. 2000 Feb 4;287(5454):873-80.

Robertson,E.J. (1987) Teratocarcinomas and Embryonic Stem Cells: A Practical Approach. IRL Press, Oxford, UK.

Russo T, Faraonio R, Minopoli G, De Candia P, De Renzis S, Zambrano N (1998) Fe65 and the protein network centered around the cytosolic domain of the Alzheimer's beta-amyloid precursor protein. FEBS Lett 434(1-2):1-7.

Russo T, Faraonio R, Minopoli G, De Candia P, De Renzis S, Zambrano N. Fe65 and the protein network centered around the cytosolic domain of the Alzheimer's beta-amyloid precursor protein. FEBS Lett. 1998 Aug 28;434(1-2):1-7.

Sabo SL, Lanier LM, Ikin AF, Khorkova O, Sahasrabudhe S, Greengard P, Buxbaum JD (1999) Regulation of beta-amyloid secretion by FE65, an amyloid protein precursor-binding protein. J Biol Chem 274(12):7952-7957.

Sabo SL, Ikin AF, Buxbaum JD, Greengard P (2001) The Alzheimer amyloid precursor protein (APP) and FE65, an APP-binding protein, regulate cell movement. J Cell Biol. 153(7):1403-1414.

Sachs AB (2000) Cell cycle-dependent translation initiation: IRES elements prevail. Cell. 101(3):243-245.

Sanger, F, Nicklen, S, and Coulson, AR (1977) DNA sequencing with chain-terminating inhibitors. Proc. Natl. Acad. Sci. U.S.A. 74, 5463-5467.

Seabrook GR, Smith DW, Bowery BJ, Easter A, Reynolds T, Fitzjohn SM, Morton RA, Zheng H, Dawson GR, Sirinathsinghji DJ, Davies CH, Collingridge GL, Hill RG. Mechanisms contributing to the deficits in hippocampal synaptic plasticity in mice lacking amyloid precursor protein.

Selkoe DJ (2001) Alzheimer's disease: genes, proteins, and therapy. Physiol. Rev 81:741-766.

Selkoe DJ (2002) Alzheimer's disease is a synaptic failure. Science 298(5594):789-791.

Selkoe DJ. Amyloid beta-protein and the genetics of Alzheimer's disease. J Biol Chem. 1996 Aug 2;271(31):18295-8.

Selkoe DJ. Toward a comprehensive theory for Alzheimer's disease. Hypothesis: Alzheimer's disease is caused by the cerebral accumulation and cytotoxicity of amyloid beta-protein. Ann N Y Acad Sci. 2000;924:17-25.

Sherrington R, Rogaev EI, Liang Y, Rogaeva EA, Levesque G, Ikeda M, Chi H, Lin C, Li G, Holman K, Tsuda T, Mar L, Foncin JF, Bruni AC, Montesi MP, Sorbi S, Rainero I, Pinessi L, Nee L, Chumekov I, Pollen D, Brookes A, Sanseau P, Polinsky RJ, Wasco W, Da Silva HAR, Haines JL, Pericak_Vance MA, Tanzi RE, Roses AD, Fraser PE, Rommens JM, St George-Hyslop PH. Cloning of a gene bearing missense mutations in early-onset familial Alzheimer's disease. Nature. 1995 Jun 29;375(6534):754-60.

Shirra MK and Hansen U. LSF and NTF-1 share a conserved DNA recognition motif yet require different oligomerization states to form a stable protein-DNA complex. J Biol Chem. 1998 Jul 24;273(30):19260-8.

Shirra MK, Zhu Q, Huang HC, Pallas D, Hansen U. One exon of the human LSF gene includes conserved regions involved in novel DNA-binding and dimerization motifs. Mol Cell Biol. 1994 Aug;14(8):5076-87.

Simeone A, Duilio A, Fiore F, Acampora D, De Felice C, Faraonio R, Paolocci F, Cimino F, and Russo T (1994) Expression of the neuron-specific FE65 gene marks the development of embryo ganglionic derivatives. Dev. Neurosci 16:53-60.

Sinha S, Lieberburg I. 1999. Cellular mechanisms of -amyloid production and secretion. Proc Natl Acad Sci USA 96: 11049-11053.

Smith-Swintosky VL, Pettigrew LC, Craddock SD, Culwell AR, Rydel RE, Mattson MP. Secreted forms of beta-amyloid precursor protein protect against ischemic brain injury.J Neurochem. 1994 Aug;63(2):781-4.

Steiner H, Fuchs S, Accili D (1997) D3 dopamine receptor-deficient mouse: evidence for reduced anxiety. Physiol Behav 63:137-141.

Stubley-Weatherly L, Harding JW, Wright JW (1996) Effects of discrete kainic acid-induced hippocampal lesions on spatial and contextual learning and memory in rats. Brain Res 716(1-2):29-38.

Sudol M, Sliwa K, Russo T. Functions of WW domains in the nucleus. FEBS Lett. 2001 Feb 16;490(3):190-195.

Tanahashi H, Asada T, Tabira T. (2002b) c954C-->T polymorphism in the Fe65L2 gene is associated with early-onset Alzheimer's disease. Ann Neurol. 52(5):691-3.

Tanahashi H, Tabira T. (1999) Molecular cloning of human Fe65L2 and its interaction with the Alzheimer's beta-amyloid precursor protein. Neurosci Lett. 261(3):143-6.

Tanahashi H, Tabira T. (2002) Characterization of an amyloid precursor protein-binding protein Fe65L2 and its novel isoforms lacking phosphotyrosine-interaction domains. Biochem J. 367(Pt 3):687-95.

Treit D, Fundytus M (1988) Thigmotaxis as a test for anxiolytic activity in rats. Pharmacol Biochem Behav 31:959-962.

Trommsdorff M, Borg JP, Margolis B, Herz J (1998) Interaction of cytosolic adaptor proteins with neuronal apolipoprotein E receptors and the amyloid precursorprotein. J Biol Chem 273(50):33556-33560.

Van Broeckhoven, C. (1998) Alzheimer's disease: Identification of genes and genetic risk factors. Prog. Brain Res. 117, 315-325.

Varvel SA, Lichtman AH (2002) Evaluation of CB1 receptor knockout mice in the Morris water maze. J Pharmacol Exp Ther 301(3):915-924.

Weidemann A, Eggert S, Reinhard FB, Vogel M, Paliga K, Baier G, Masters CL, Beyreuther K, Evin G. (2002) A novel epsilon-cleavage within the transmembrane domain of the Alzheimer amyloid precursor protein demonstrates homology with Notch processing. Biochemistry. 41(8):2825-35.

Weisgraber KH, Mahley RW. Human apolipoprotein E: the Alzheimer's disease connection. FASEB J. 1996 Nov;10(13):1485-94.

Wilson RI, Nicoll RA (2002) Endocannabinoid signaling in the brain. Science 296(5568):678-682.

Wiltfang J, Smirnov A, Schnierstein B, Kelemen G, Matthies U, Klafki HW, Staufenbiel M, Huther G, Ruther E, Kornhuber J (1997) Improved electrophoretic separation and immunoblotting of beta-amyloid (A beta) peptides 1-40, 1-42, and 1-43. Electrophoresis 18(3-4):527-532.

Wong ST, Athos J, Figueroa XA, Pineda VV, Schaefer ML, Chavkin CC, Muglia LJ, Storm DR. (1999) Calcium-stimulated adenylyl cyclase activity is critical for hippocampus-dependent long-term memory and late phase LTP. Neuron 23(4):787-798.

Xiang H, Hochman DW, Saya H, Fujiwara T, Schwartzkroin PA, Morrison RS (1996) Evidence for p53-mediated modulation of neuronal viability. J Neurosci 16(21):6753-6765.

Xu DH, Sato C, Rogaev E, Smith M, Janus C, Zhang Y, Aebersold R, Farrer LS, Sorbi S, Bruni A, Fraser P, St George-Hyslop P. Nicastrin modulates presenilin-mediated notch/glp-1 signal transduction and betaAPP processing. Nature. 2000 Sep 7;407(6800):48-54.

Yamazaki T, Koo EH, Selkoe DJ. Cell surface amyloid beta-protein precursor colocalizes with beta 1 integrins at substrate contact sites in neural cells. J. of Neurosc. 1997 Feb; 17 (3): 1004-1010.

Yankner BA. The pathogenesis of Alzheimer's disease. Is amyloid beta-protein the beginning or the end? Ann N Y Acad Sci. 2000;924:26-8.

Yu C, Kim SH, Ikeuchi T, Xu H, Gasparini L, Wang R, Sisodia SS. (2001) Characterization of a presenilin-mediated amyloid precursor protein carboxyl-terminal fragment gamma. Evidence for distinct mechanisms involved in gamma -secretase processing of the APP and Notch1 transmembrane domains. J Biol Chem. 276(47):43756-60.

Yu G, Nishimura M, Arawaka S, Levitan D, Zhang L, Tandon A, Song YQ, Rogaeva E, Chen F, Kawarai T, Supala A, Levesque L, Yu H, Yang DS, Holmes E, Milman P, Liang Y, Zhang DM, Xu DH, Sato C, Rogaev E, Smith M, Janus C, Zhang Y, Aebersold R, Farrer LS, Sorbi S, Bruni A, Fraser P, St George-Hyslop P. (2000) Nicastrin modulates presenilin-mediated notch/glp-1 signal transduction and betaAPP processing Nature (London) 407, 48-54.

Zambrano N, Buxbaum JD, Minopoli G, Fiore F, De Candia P, De Renzis S, Faraonio R, Sabo S, Cheetham J, Sudol M, Russo T (1997) Interaction of the phosphotyrosine interaction/phosphotyrosine binding-related domains of Fe65 with wild-type and mutant Alzheimer's beta-amyloid precursor proteins. J Biol Chem 272(10):6399-6405.

Zambrano N, Minopoli G, de Candia P, Russo T (1998) The Fe65 adaptor protein interacts through its PID1 domain with the transcription factor CP2/LSF/LBP1. J Biol Chem 273(32):20128-20133.

Zambrano N, Bruni P, Minopoli G, Mosca R, Molino D, Russo C, Schettini G, Sudol M, Russo T (2001) The beta-amyloid precursor protein APP is tyrosine-phosphorylated in cells expressing a constitutively active form of the Abl protoncogene. J Biol Chem 276(23):19787-19792.

Zheng JB, Kimberly WT, Selkoe DJ (2002) Amyloid precursor protein intracellular domain (AICD) is present in mouse brain and primary neurons. Abstract for 32nd annual SFN meeting.

Zheng P, Eastman J, Vande Pol S, Pimplikar SW. PAT1, a microtubule-interacting protein, recognizes the basolateral sorting signal of amyloid precursor protein. Proc Natl Acad Sci U S A. 1998 Dec 8;95(25):14745-50.

Zhou QY, Quaife CJ, Palmiter RD (1995) Targeted disruption of the tyrosine hydroxylase gene reveals that catecholamines are required for mouse fetal development. Science 374:640-643.

Vita

Baiping Wang

EDUCATION:

MD. Beijing Medical University. 1996

Ph.D. University of Washington. 2003

PUBLICATIONS:

Wang B, Hu Q, Hearn MG, Shimizu K, Ware CB, Liggitt DH, Jin L-W, Cool BH, Storm DR, Martin GM. Isoform Specific FE65 knockout Leads to Impaired learning and memory. Submitted to *J. Neuroscience. Res.* 2003

Hu Q, Cool B, Wang B, Hearn MG, Martin GM. (2002) A candidate molecular mechanism for the association of an intronic polymorphism of FE65 with resistance to very-late onset dementia of the Alzheimer type. *Human Mol. Genetics*. 2002, 11:4.

Maezawa I, Wang B, Hu Q, Martin GM, Jin L-W and Oshima J. Alterations of chaperone protein expression in presenilin mutant neurons in response to glutamate excitotoxicity. *Pathology International*. 2002 Sep;52(9):551-4.

HONOR:

Glenn foundation/American Federation for Aging Research Scholarship